In situ Synthesis of Gel Polymer Electrolytes for Lithium Batteries

Xiangran Cheng,[a] Yi Jiang,[a] Chenhao Lu,[a] Jiaxin Li,[a] Jiahe Qu,[a] Bingjie Wang,*[a] and Huisheng Peng*[a]

Gel polymer electrolytes (GPEs) are considered as a promising solution to replace organic liquid electrolytes for safer lithium (Li) batteries due to their high ionic conductivity comparable to liquid electrolytes, no risk of leakage, and high flexibility. However, poor interfacial contact between electrodes and GPEs leads to high interfacial impedance and unsatisfactory electrochemical performance. The emerging *in situ* synthesized GPEs can fully infiltrate into porous electrodes and form intimate interfaces, improving interfacial contact and electrochemical performance. This perspective covers recent advances of *in situ* GPEs in design, synthesis, and applications in lithium (Li) batteries. Polyester and polyether-based GPEs are mainly discussed followed by a brief introduction of GPEs with other polymer matrices, such as poly(ionic liquid)s, cyanoethyl polyvinyl alcohol, poly(vinyl acetal) and single-ion conductors. Then, the recent progress in Li batteries using *in situ* GPEs are summarized, including Li-ion battery, Li-metal battery, Li-sulfur battery, and Li-air battery. Finally, the remaining challenges and future perspectives of *in situ* GPEs are discussed. We hope this perspective can offer guidance for *in situ* synthesis of GPEs and facilitate their applications in high-performance Li batteries.

1. Introduction

Nowadays, lithium (Li-)ion batteries have become one of the most promising energy storage devices due to their high operating voltage, high energy density, long cycle life, low self-discharge rate, and no memory effect.[1] Electrolytes, an important part of Li-ion battery, can transport ions and conduct current between positive and negative electrodes. Designing suitable electrolytes is one of the key factors in realizing Li-ion batteries with high energy and power densities, long cycle life, and high safety. The state-of-art Li-ion batteries usually use liquid electrolytes for their high ionic conductivity and effective contact with porous electrodes, but liquid electrolytes face the risks of leakage and volatilization, which can cause the battery to burn and even explode.[2]

Solid-state electrolytes, including inorganic solid electrolytes and solid polymer electrolytes, have been developed to tackle the problems of liquid electrolytes. Despite of their high ionic conductivity, inorganic solid electrolytes have not been widely used in Li batteries due to their brittleness and poor electrode/electrolyte interfacial contact. Solid polymer electrolytes are composed of polymer matrix and Li salts, and Li-ions migrate through repeated coordination-dissociation processes. However, typical solid polymer electrolytes such as poly-ethylene oxide (PEO) exhibit low ionic conductivity (10^{-8}–10^{-6} S/cm) at room temperature, orders of magnitude lower than the practical requirements (10^{-4}–10^{-3} S/cm).[3] To improve ionic conductivity, Feuillade et al. first proposed adding plasticizers to polymer electrolytes in the 1970s, thus promoting the development of gel polymer electrolytes (GPEs).[4]

GPEs are usually composed of polymer matrix, organic solvent, and electrolyte salt. The polymer networks prevent electrolyte leakage and provide mechanical support, while the solvents dissolve the salts and transport Li-ions. GPEs combine the advantages of high ionic conductivity (10^{-3}–10^{-2} S/cm), enhanced safety, and good flexibility and processability, exhibiting great potential for large-scale production. However, the quasi-solid state GPEs are usually prepared before battery assembly and have difficulty in fully permeating into the porous electrodes (e.g., solution-casting, phase-inversion, and electrospinning), leading to poor interfacial contact and high interface impedance (Figure 1a).[5] Moreover, the complicated *ex situ* methods are always accompanied by the volatilization of organic solvents, which is harmful to the environment. *In situ* synthesis of GPEs, which is cured from liquid gel precursor within the battery, is proposed to solve this challenge.[6] The gel precursor solutions are typically composed of monomers, plasticizers, Li salts, and initiators, which are injected into the battery and cured *in situ* under certain external conditions,

[a] X. Cheng,+ Y. Jiang,+ Dr. C. Lu, J. Li, J. Qu, Prof. B. Wang, Prof. H. Peng
State Key Laboratory of Molecular Engineering of Polymers
Department of Macromolecular Science and
Laboratory of Advanced Materials
Fudan University
Shanghai 200438 (China)
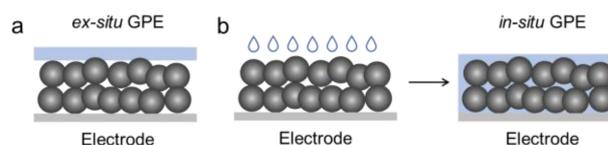E-mail: wangbingjie@fudan.edu.cn
        penghs@fudan.edu.cn

Figure 1. Schematic of *ex situ* GPE and *in situ* GPE.

such as ultraviolet irradiation and heating (Figure 1b).[7] Therefore, in situ preparing GPEs for solid-state Li batteries has attracted increasing attention.[8]

Excellent reviews are available discussing different synthesis conditions of *in situ* GPEs, such as UV-irradiation, heating, room-temperature, and initiator-free.[7,9] A few available reviews discussed polymerization mechanisms, such as free radical polymerization, cationic polymerization, anionic polymerization, and electrochemical initiated polymerization.[7,10] However, the structures of polymer host significantly influence the overall performance of GPEs and batteries, including ionic conductivity, mechanical properties and thermal stability, but few reviews thoroughly discuss the structure and properties of different polymer hosts for *in situ* GPEs, and the functionalities of *in situ* GPEs in different Li batteries.

This perspective comprehensively summarizes the functional design and advanced applications of *in situ* GPEs for Li batteries. We first introduce two kinds of typical polyester and polyether GPEs in detail, followed by a brief introduction of other GPEs, such as poly(ionic liquid)s, cyanoethyl polyvinyl alcohol, poly(vinyl acetal), and single-ion conductor. The recent advances for *in situ* GPEs in various Li batteries, including Li-ion battery, Li-metal battery, Li-sulfur battery, and Li-air battery, are then systematically presented. Finally, the key challenges and prospects for *in situ* GPEs are discussed. This perspective aims to summarize the basic knowledge of the *in situ* synthesized GPEs and inspire more researchers to find solutions to construct safer and high-performance Li batteries.

2. Polyester

Carbonyl-containing polymers, such as polyacrylates and polycarbonates, have strong interactions with the oxygen groups in carbonate solvents, thus exhibiting high electrolyte absorption and excellent ionic conductivity. They are usually synthesized *in situ* by free radical polymerization of monomers, such as methyl methacrylate (MMA),[11] butyl acrylate (BA),[12] butyl ethoxylated trimethylolpropane triacrylate (ETPTA),[13] pentaerythritol tetraacrylate (PETEA),[14] vinylene carbonate (VC)[15] and vinyl ethylene carbonate (VEC),[16] or crosslinking of oligomers, such as poly(ethylene glycol) methyl ether acrylate (PEGMEA),[17] poly (ethylene glycol)diacrylate (PEGDA).[18] In this Section, polyester-based GPEs are classified into polyacrylates and polycarbonates based on polymer matrix, and different modification strategies are introduced.

2.1. Polyacrylate

Among polyacrylates, PMMA is the most common polymer matrix of GPEs for Li batteries. Because of the strong interactions between the $-C=O$ group in acrylate and the O atom in carbonate solvent, PMMA provides excellent liquid absorption capability. For example, the crosslinked GPEs by *in situ* polymerizing MMA and PEGDMA in ethylene carbonate/propylene carbonate liquid electrolytes initiated by azodiisobutyronitrile (AIBN) (Figure 2a).[11a] The low viscosity precursor solution mainly made of MMA could efficiently wet porous

Xiangran Cheng is currently a Ph.D. student at the Department of Macromolecular Science at Fudan University. She received her B.S. degree in chemical engineering from Dalian University of Technology in 2019. Her work focuses on flexible energy storage devices and their applications in energy storage textile systems.

Yi Jiang is currently a Ph.D. student at the Department of Macromolecular Science at Fudan University. She received her B.S. degree in polymer material and engineering from Harbin Institute of Technology in 2021. Her work focuses on flexible lithium-ion batteries and their applications in energy storage textiles.

Bingjie Wang is an associate professor at the Laboratory of Advanced Materials at Fudan University. He received his B.E. degree in polymer materials and engineering from Sichuan University in 2009, a Ph.D. degree from Ningbo Institute of Materials Technology and Engineering. Chinese Academy of Sciences in 2014. His research focuses on flexible energy storage devices.

Huisheng Peng is currently a university professor at the Department of Macromolecular Science and Laboratory of Advanced Materials at Fudan University. He received his B.E. in polymer materials at Donghua University in China in 1999, his M.S. in macromolecular chemistry and physics at Fudan University in China in 2003, and his Ph.D. in Chemical Engineering at Tulane University in the USA in 2006. He then worked at Los Alamos National Laboratory before joining Fudan University in 2008. He focuses on the new direction of fiber electronics.
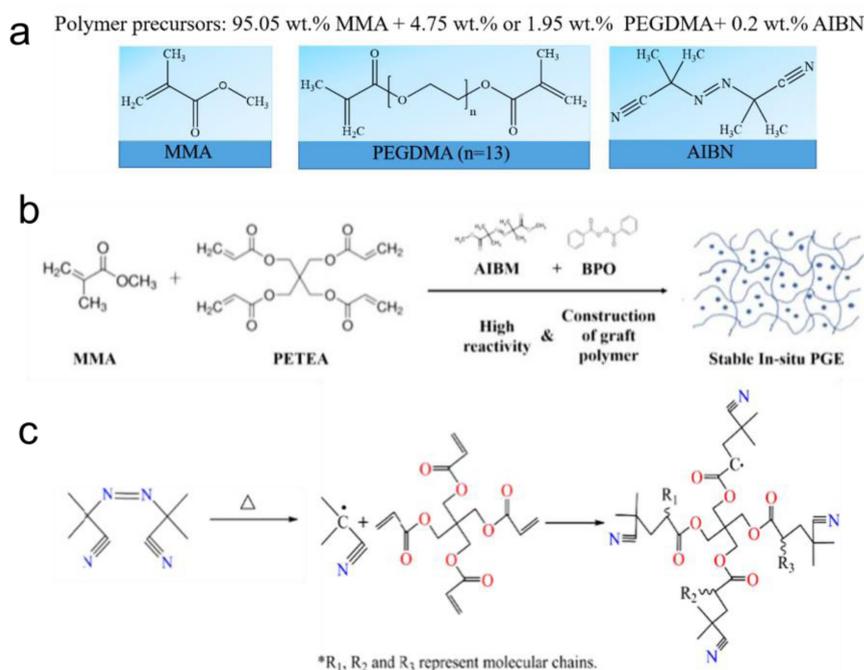
Batteries & Supercaps

Perspective
doi.org/10.1002/batt.202300057

Chemistry Europe
European Chemical
Societies Publishing

Figure 2. a) Preparation procedures for PMMA-based GPEs. Reproduced with permission from Ref. [11a]. Copyright (2020) Elsevier. b) Preparation of PMMA-based GPEs initiated by compound initiators. Reproduced with permission from Ref. [11b]. Copyright (2022) Elsevier. c) Polymerization of PETEA-based GPEs. Reproduced with permission from Ref. [14a]. Copyright (2016) Elsevier.

electrodes. After polymerization, PMMA was well-compatible with carbonate-based liquid electrolytes and showed a high conductivity of 3.9×10^{-3} S/cm at 20 °C. The free radical polymerization is normally triggered by AIBN, benzoyl peroxide (BPO), or 2-hydroxy-2-methylpropiophenone (HMPP). However, these initiators often decompose incompletely after the polymerization, and the remaining radicals cause side reactions during the following charge-discharge process. Compound initiators employing dimethyl azodiisobutyrate (AIBM) and BPO could regulate the initiation process (Figure 2b).[11b] The as-prepared GPEs exhibited a high Li$^+$ conductivity and good cyclic stability in Gr/NCM811 pouch batteries with a capacity retention of 91.1% after 600 cycles.

ETPTA[13] and PETEA[14] have multiple vinyl bonds at the end of the chain. After polymerization, their highly crosslinked networks exhibit high mechanical strength and compatibility with liquid electrolytes. An ETPTA-based GPE was prepared by polymerizing ETPTA and HMPP in 2 mol/L LiTFSI in triethyleneglycoldimethylether (TEGDME).[13] Through in situ polymerization method, plasticizers were uniformly distributed in the crosslinked polymer network, and intimate electrolyte/electrode interface was formed, facilitating fast Li$^+$ transport both in bulk and at the interface. Similarly, a PETEA-based GPE was synthesized with a high ionic conductivity of 1.13×10^{-2} S/cm for a Li-sulfur battery (Figure 2c).[14a] By encapsulating the liquid electrolyte in the cross-linked polymer network, the dissolution and diffusion of polysulfides were constrained. The resulting Li-sulfur battery exhibited enhanced rate capacity and cycle stability.

Low molecular chain polymers, such as PEGDA[18] and PEGMEA[17,19] are usually used as crosslinkers or copolymers for

in situ GPEs. Low molecular chain polymers with good fluidity can infiltrate into the porous electrode and maintain full contact with electrodes after in situ gelation. Their linear —CH$_2$—CH$_2$—O— segments also show good flexibility. An in situ polymerized GPE was synthesized via thermal polymerization of PEGDA and ETPTA.[18c] The PEGDA monomer had one double bond, while ETPTA monomer had three double bonds in each unit. In GPEs, PEGDA monomer polymerized to produce linear segments and ETPTA monomer polymerized to form bulk segments. The as-obtained GPEs encapsulated a large amount of liquid electrolytes and manifested a high ionic conductivity of 8.7×10^{-4} S/cm. The in situ crosslinked PEGDA-based GPE was used for Li-air battery (Figure 3a).[18d] LiTFSI and SN were dissolved in liquid-state PEGDA to form a homogeneous precursor solution. Then the precursor was heated at 60 °C and crosslinked into solid-state GPEs catalyzed by AIBN. Compared with high-molecular-weight polymers, such as PEO and PVDF-HFP, liquid PEGDA with good fluidity could wet electrodes sufficiently and form compact interface between anode and electrolyte. A series of GPEs were in situ prepared via the crosslinking reaction between poly(ethylene glycol) methyl ether methacrylate and di-methacrylate, and the relationship between crosslinking density and electrochemical performance of GPEs was further investigated (Figure 3b).[19b] With increasing crosslinking density, polymer network could encapsulate carbonate electrolytes and suppress the side reaction between electrolyte and Li metal. However, highly crosslinked polymer network also lowered the polymer chain flexibility and the carbonate electrolytes diffusivity. By adjusting the length of linear chain, the GPEs with optimized crosslinking density could achieve desired battery performance.
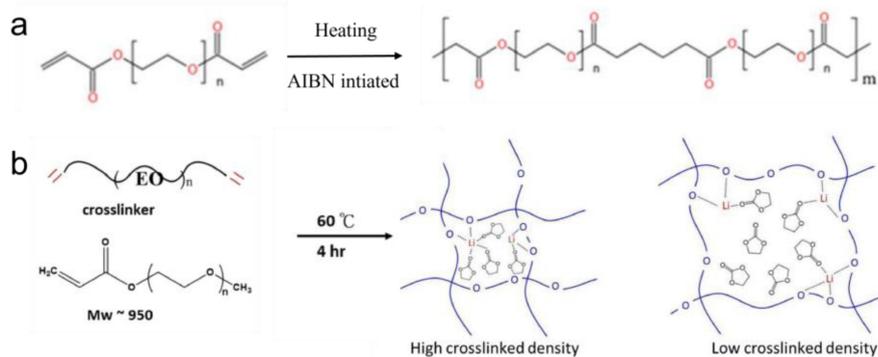
Figure 3. a) Schematic of Li$^+$ transfer in PEGDA-LiTFSI-SN polymer electrolytes. Reproduced with permission from Ref. [18d]. Copyright (2022) IOP Publishing Ltd. b) Synthesis of polyether di-methacrylate crosslinker and GPEs and illustration of the interaction of Li$^+$, EC and polymer matrix with different crosslinking density. Reproduced with permission from Ref. [19b]. Copyright (2020) Elsevier.

Designing heteroatoms-containing polymer backbones is an efficient strategy to improve the performance of GPEs. F-contained polymer matrix can form sable SEI layer on Li metal and improve oxidation stability towards cathodes. A hybrid polymer framework of PEGDMA and trifluoroethyl methacrylate (TFMA).[20] The $-CF_3$ groups in the polymer skeleton could react with Li$^+$ and form a stable LiF-rich SEI to protect Li metal anode. Besides, the C–F bond, as one of the strongest single bonds in organic compounds, has outstanding high-voltage resistance.[21] A poly(maleic anhydride-hexafluorobutyl methacrylate-methyl methacrylate) (PMHM) electrolyte was in situ polymerized, and exhibited a high electrochemical stability window of 5.5 V vs. Li/Li$^+$ and ionic conductivity of 1.1×10^{-3} S/cm (Figure 4a).[22] The superior high-voltage stability and fast ion migration dynamics were attributed to C–F and ester/acid anhydride groups in the polymer chain. Boron with a vacant p-orbital can interact with the anions of electrolyte salts and increase the dissociation of ion pairs. Therefore, the boron-containing polymer matrix for GPE exhibits high ionic conductivity and Li$^+$ transference number. A boron-containing GPE by polymerizing a cyclic boron ester and branched boron ester into the 3D structure (Figure 4b).[23] Incorporated with anion-trapping boron moieties, the GPEs presented a high ionic
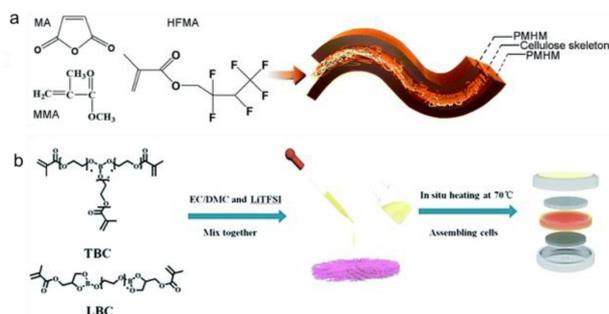
conductivity (8.4×10^{-4} S/cm) and near single ion conduction (Li$^+$ transference number of 0.76).

In addition, copolymerization and blend can improve the ionic conductivity and mechanical strength of polyacrylate-based GPEs.[24] A novel densely-packed multifunctional GPE by in situ copolymerization of pentaerythritol tetraacrylate (PETEA) and 2-hydroxyethyl acrylate (HEA) via a thermal initiation method (Figure 5a).[25] The self-polymerization of PETEA formed randomly stacked polymer skeleton. In contrast, copolymerized GPEs constructed a 3D polymer microsphere network structure, owing to the strong hydrogen bonding between the hydroxyl groups on the end of polymer chains. This copolymer structure provided uniform channels for Li$^+$ migration and promoted

Figure 4. a) Synthesis of in situ GPEs from MA, HFMA and MMA monomers. Reproduced with permission from Ref. [22]. Copyright (2021) Royal Society of Chemistry. b) Synthesis of the borate-rich GPEs via in situ polymerization of linear boron ester and branched boron ester. Reproduced with permission from Ref. [23]. Copyright (2019) Royal Society of Chemistry.
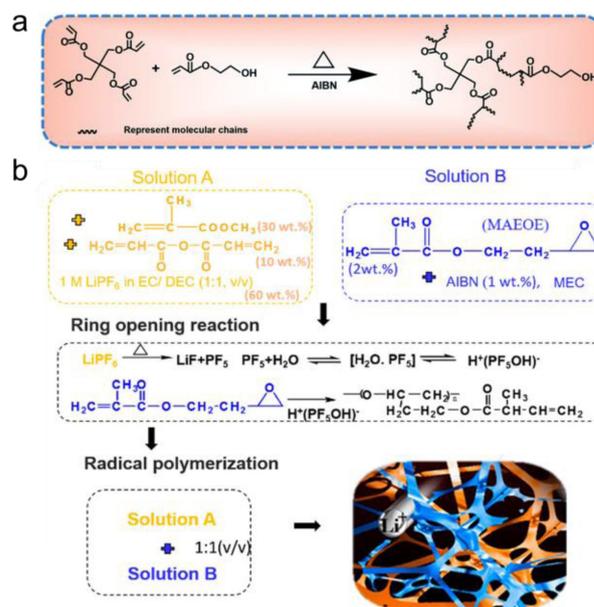

Figure 5. a) Synthesis of the crosslinked GPE matrix by in situ copolymerization of pentaerythritol tetraacrylate (PETEA) and 2-hydroxyethyl acrylate (HEA) via a thermal initiation method. Reproduced with permission from Ref. [25]. Copyright (2022) Royal Society of Chemistry. b) Copolymerization mechanism of acrylic anhydride and methyl methacrylate. Reproduced with permission from Ref. [27]. Copyright (2017) American Chemical Society.

Batteries & Supercaps

Perspective
doi.org/10.1002/batt.202300057

Chemistry
Europe
European Chemical
Societies Publishing

uniform Li plating. Besides, a GPE rich in ester groups was synthesized by using PETEA crosslinked with divinyladipate for Li-sulfur batteries.[26] Combining PETEA and ester could improve the flexibility of the polymer matrix. Meanwhile, large ester groups in polymer skeleton could capture polysulfide and enable stable cycling of Li-sulfur batteries. A rigid crosslinked polymer network was *in situ* prepared with acrylic anhydride, methyl methacrylate and crosslinking agent 2-methyl-acrylic acid-2-oxirane-ethyl ester (Figure 5b).[27] The anhydride and acrylate groups provided high voltage resistance and ionic conductivity, respectively. The as-prepared poly(acrylic anhydride) and poly(methyl methacrylate)-based GPEs exhibited an electrochemical stability window exceeding 5 V *vs.* Li/Li$^+$, ionic conductivity of 6.79×10^{-4} S/cm at room temperature and high mechanical strength of 27.5 MPa.

Composite GPEs also play a great role in the development of polyacrylate-based GPEs. Inorganic fillers, such as SiO$_2$,[28] Al$_2$O$_3$,[29] LATP,[30] LLZO[31]) and organic fillers polyacrylonitrile (PAN)[32] and cellulose acetate (CA),[33] have been used in GPEs. A SiO$_2$-composite GPE was prepared *via in situ* polymerization of tripropylene gycol diacrylate (TPGDA) monomer in a SiO$_2$ hollow nanosphere layer (Figure 6a).[28] The polymerized TPGDA framework eliminated safety risks caused by electrolyte leakage. The SiO$_2$ layer provided the GPEs with enhanced mechanical strength and high room-temperature ionic con-

ductivity. *In situ* polymerized GPE also addressed the rigid interfaces between inorganic solid electrolytes and electrodes. Introducing *in situ* GPE between the garnet LLZO and the electrodes could address the rigid electrode/electrolyte interface and construct a continuous ion conduction network.[31c]

PAN electrospun membrane is a common supporting skeleton for GPEs, offering favorable oxidation resistance and mechanical properties. PETEA monomers were *in situ* polymerized in a PAN membrane to obtain GPEs (Figure 6b).[32a] The as-fabricated GPEs possessed a high Li$^+$ transference number of 0.77 and electrochemical decomposition voltage of 5.15 V. PETEA and PAN could synergistically promote Li$^+$ transportation and stable charge-discharge performance of batteries by constructing fast ion transport channels. CA membrane with abundant ether and ester functional groups shows good affinity to the electrolyte. A composite GPE was prepared with CA as a matrix, PEGDA as a crosslinking agent, and layered boron nitride (BN) as reinforcement for Li-ion batteries.[33b] Due to the interaction with anions in liquid electrolyte and the polymer matrix, BN filler could facilitate Li$^+$ transport and improve the oxidative stability of the GPE. Combining polar groups in CA and Lewis acid-base characteristic of BN together, the obtained GPE exhibited a high ionic conductivity of 8.9×10^{-3} S/cm at 30 °C and an excellent electrochemical stability up to 5.5 V.
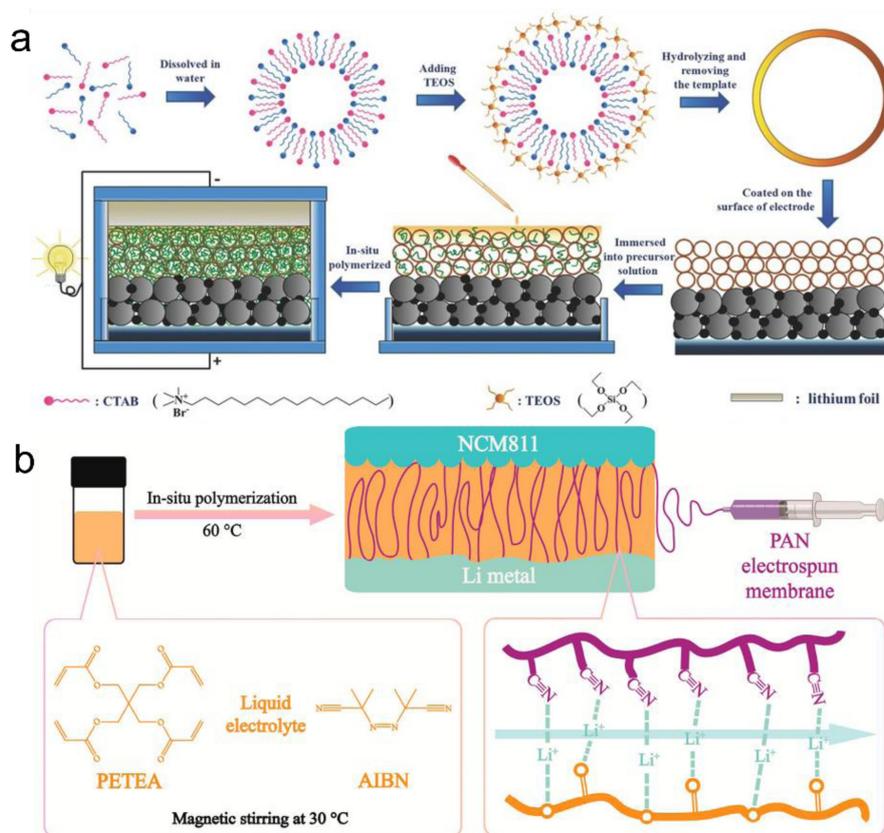

Figure 6. a) Schematic illustration for the preparation route of SiO$_2$ composite GPEs *via in situ* polymerizing the tripropylene gycol diacrylate (TPGDA) in a SiO$_2$ hollow nanosphere layer. Reproduced with permission from Ref. [28]. Copyright (2016) Wiley-VCH. b) Fabrication process of pentaerythritol tetraacrylate (PETEA)-based GPEs in a polyacrylonitrile (PAN) membrane. Reproduced with permission from Ref. [32a]. Copyright (2022) American Chemical Society.

Batteries & Supercaps

Perspective
doi.org/10.1002/batt.202300057

**Chemistry
Europe**
European Chemical
Societies Publishing

Organic solvents play an important role as Li$^+$ transport medium in GPEs, but they are unstable at high temperatures and may catch fire or even explode under abusive conditions. To address safety concerns, ionic liquids have been incorporated into GPEs to replace organic solvent, called "ionogels".[34] Ionic liquids are molten salts at room temperature, consisting of weakly coordinated cations and anions. They are considered as "green" solvents because of nonflammability, negligible vapor pressure, high ionic conductivity, wide electrochemical window, and high thermal stability.[35] An ionic liquid-based GPE was prepared *via in situ* polymerization of trimethylolpropane trimethylacrylate in tributylmethylammonium bis(trifluoromethanesulfonyl) imide (N$_{1,4,4,4}$TFSI). The N$_{1,4,4,4}$TFSI ionic liquid could effectively dissociate the Li salts and facilitate ion transport. The as-prepared GPE delivered a high ionic conductivity of 6.15×10^{-3} S/cm at 25 °C and enhanced interface stability with Li metal electrode. Besides, solvent ionic liquids consisting of equimolar glyme and Li salts have also been reported. A novel ionogels by UV-induced polymerization of butyl acrylate in a solvate ionic liquid ([Li(G4)][TFSI]) (Figure 7a).[36] Almost all the glyme molecules were complexed with Li$^+$, leaving TFSI$^-$ anions uncoordinated to Li$^+$. The obtained GPEs exhibited a high Li$^+$ transference number of 0.46.

Flame-inhibiting additives can also effectively mitigate the safety risks of batteries. Among them, organic alkyl phosphates possess excellent fire-extinguishing capability, low density, low viscosity, and the capability to dissolve Li salts.[37] During heating, phosphonates generate free radicals P$^\bullet$ and remove H$^\bullet$ or O$^\bullet$ radicals derived from organic solvents, thereby terminating the chain reaction of free radicals and retarding combustion. A new non-flammable elastic poly(butyl acrylate) (PBA)-based GPE with the addition of trimethyl phosphate (TMP).[37a] TMP rendered the electrolyte non-flammable. Compared with the methyl side group, the large butyl side group of PBA provided more free volume and facilitated the movement of
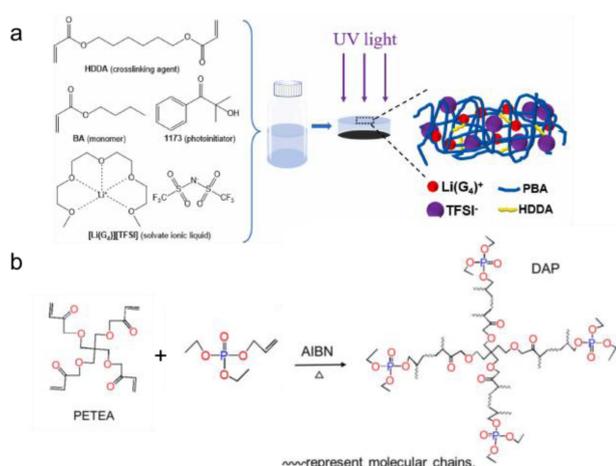
polymer chains, thus endowing the GPE with better flexibility and elasticity. Besides, incorporating the P atom into the polymer backbone also improved the safety of GPEs.[38] A non-flammable GPE was *in situ* synthesized *via* copolymerization of diethyl allyl phosphate (DAP) monomer and pentaerythritol tetraacrylate (PETEA) crosslinker in an all-fluorinated electrolyte (Figure 7b).[38c] The as-fabricated GPEs possessed high ionic conductivity (2×10^{-3} S/cm) and enhanced safety (nonflammable and free of liquid leakage).

Because self-healing GPEs can repair defects and voids at the electrode/electrolyte interface, they have been developed to improve battery performance. By copolymerization of 2-(3-(6-methyl4-oxo-1,4-dihydropyrimidin-2-yl)ureido)ethyl methacrylate (UPyMA) and acrylates, self-healing GPEs have been prepared (Figure 8a).[39] The self-healing behavior was attributed to intramolecular hydrogen bonding between the ester groups and urea groups in the UPyMA units of the polymer chains (Figure 8b). Additionally, the GPE also showed high mechanical elasticity due to hydrogen bonds interactions. These characteristics endowed the Li metal anode with an adaptable Li electrode/electrolyte interface, which was stable against the repeated electrode volume change and crack growth during cycling.

2.2. Polycarbonate

Polycarbonates have been developed as polymer electrolytes to overcome the safety problems of carbonate liquid electrolytes. The polar carbonate groups in polymer skeletons benefit salt dissociation and ion solvation. Vinyl ethylene carbonate (VEC) with a unique framework containing C=C and C=O bonds can be polymerized *via* C=C bonds. The weak complexation between Li$^+$ and C=O bonds in the polymer backbone can facilitate ion dissociation and transport. VEC also shows high stability towards Li metal anode. A novel dual-salt GPE was
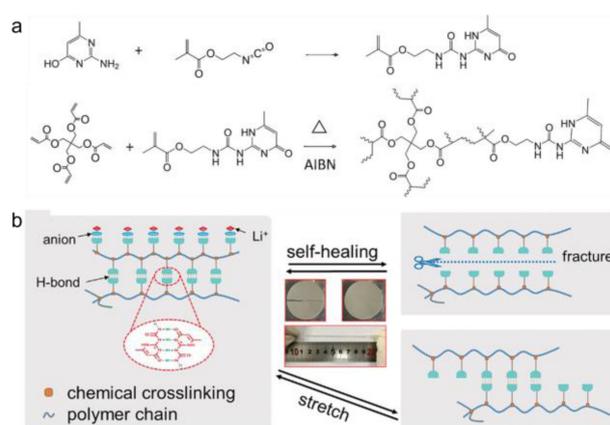

Figure 7. a) Synthetic procedure of [Li(G4)][TFSI] ionogels. Reproduced with permission from Ref. [36]. Copyright (2022) Elsevier. b) *In situ* copolymerization mechanism of diethyl allyl phosphate (DAP) and pentaerythritol tetraacrylate (PETEA) monomers. Reproduced with permission from Ref. [38c]. Copyright (2021) Springer Nature.

Figure 8. a) Reaction route to synthesize the 2-(3-(6-methyl4-oxo-1,4-dihydropyrimidin-2-yl)ureido)ethyl methacrylate (UPyMA) monomer and self-healing GPEs. Reproduced with permission from Ref. [39a]. Copyright (2020) Wiley-VCH. b) Schematic diagram of the self-healing mechanism and elasticity. Reproduced with permission from Ref. [39b]. Copyright (2022) Wiley-VCH.

synthesized *via in situ* polymerization of VEC and PETEA in a PVDF-HFP porous structure (Figure 9a).[16] The GPEs showed high ionic conductivity of 6.9×10^{-3} S/cm at room temperature, Li^+ transference number of 0.512, oxidative resistance of 5.3 V *vs.* Li/Li^+ and favorable interfacial compatibility. To enhance the safety of GPEs, vinylene carbonate (VC) was *in situ* polymerized in a 3D electrospun PVDF nanofiber membrane embedded with silane-functionalized LATP nano-particles(Si@LATP) (Figure 9b).[15] The high dielectric PVDF embedded with Si@LATP particles greatly enhanced Li^+ transport in bulk GPE. The *in situ* solidification process accelerated the Li^+ transport across the electrode/electrolyte interface. The resulting composite GPE exhibited superior ionic conductivity (1.06×10^{-3} S/cm at 25 °C), near single-ion conducting characteristic (Li^+ transference number = 0.82), good mechanical strength (tensile strength = 15.3 MPa) and high-voltage endurance (4.86 V).

3. Polyether

Polyester-based GPEs are usually synthesized *in situ via* a free radical mechanism, which requires extra non-electrolytic monomers and initiators and special conditions, such as high temperature and UV irradiation. The external initiators and residual monomers may cause side reactions and degrade battery performance during long cycles. To adapt to the industrial production of batteries, it is necessary to develop *in situ* synthesis strategies performed under moderate external conditions without introducing impurities. Recently, polyether-based GPEs have been *in situ* synthesized *via* ring-opening polymerization of cyclic ether[40] or crosslinking of linear ether oligomers[41] catalyzed by Li salts under room temperature.
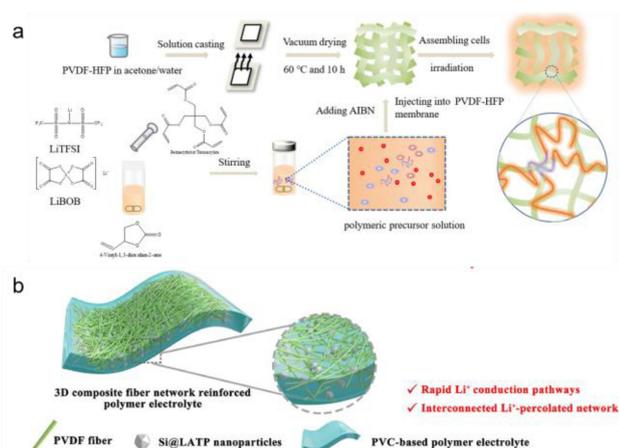
3.1. Ring-opening polymerization of cyclic ether

Cyclic ethers, such as 1,3-dioxolane (DOL), are common solvents for Li metal batteries due to their high reduction stability. However, they exhibit poor oxidation stability and high flammability. Conversing liquid ether electrolytes into polyether electrolytes can improve safety and oxidative stability. Lithium hexafluorophosphate ($LiPF_6$) was used to initiate the cationic polymerization of 1,3-dioxolane (DOL) in 1,2-dimethoxyethane (DME) liquid electrolytes at room temperature (Figure 10a).[40a] This facile synthesis strategy exhibited several advantages including free of impurities and moderate conditions.

Other initiators, such as lithium difluoro (oxalato)borate (LiDFOB),[42] tin trifluoromethanesulfonate ($Sn(OTf)_2$),[43] magnesium trifluoromethanesulfonate ($Mg(OTf)_2$),[44] and tris-(1,1,1,3,3,3-hexafluoroisopropyl) (HFiP)[45] have also been developed. Besides, a small amount of LiDFOB with 2 M lithium bis(trifuoromethylsulfonyl)imide (LiTFSI) was applied to construct a dual-salt polyDOL-based GPE.[42a] The redox reactions of two anions of double salts with Li metal formed nitrogen, fluoride and boron-rich solid electrolyte interphase (SEI) and cathode electrolyte interphase (CEI), which could inhibit dendrite growth and improve cell lifespan. When using $Sn(OTf)_2$ as the initiator, Sn^{2+} attached to the oxygen atom of DOL and initiated the ring-opening polymerization of DOL (Figure 10b). Meanwhile, Sn^{2+} was reduced to metallic Sn and formed a thin Li-Sn alloy layer on the surface of Li metal.[43a] The Li-Sn alloy layer improved surface charge transference and deposited Li density. Similarly, $Mg(OTf)_2$ was reduced to Mg metal and distributed uniformly on the Li metal surface while initiating the polymerization of DOL.[44] Trace Mg element in SEI layer could adjust space charge distribution and inhibit dendrite growth on Li metal surface. After initiating DOL polymerization,
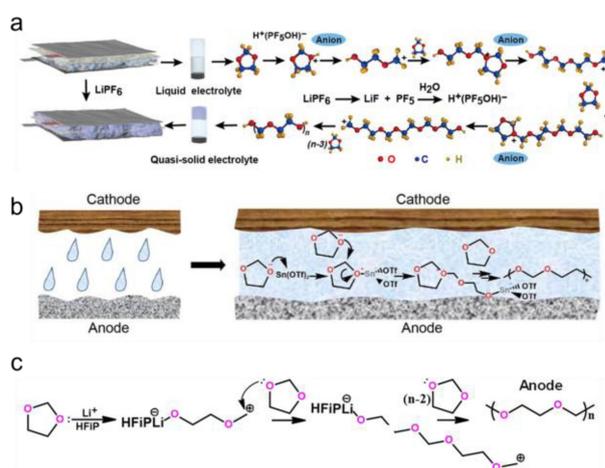

Figure 9. a) Reaction route to obtain the poly (vinyl ethylene carbonate)-based dual-salt GPE. Reproduced with permission from Ref. [16]. Copyright (2022) Elsevier. b) Schematic illustration of 3D composite fiber network reinforced poly (vinylene carbonate)-based GPEs. Reproduced with permission from Ref. [15]. Copyright (2022) Elsevier.

Figure 10. a) Schematic of the polymerization mechanism of DOL induced by $LiPF_6$. Reproduced with permission from Ref. [40a]. Copyright (2018) IOP Publishing Ltd. b) Schematic illustrating *in situ* polymerization mechanism of DOL induced by $Sn(OTf)_2$ and the following formed tin protected Li layer. Reproduced with permission from Ref. [43a]. Copyright (2022) Elsevier. c) Reaction mechanism of HFiP and DOL. Reproduced with permission from Ref. [45]. Copyright (2021) American Chemical Society.

Batteries & Supercaps

Perspective
doi.org/10.1002/batt.202300057

Chemistry
Europe
European Chemical
Societies Publishing

HFiP decomposed into the $-CF_3$ functional groups and formed a dense CEI layer to improve the battery lifetime (Figure 10c).[45]

Copolymerization and blending are common strategies to modify the properties of polyether-based GPE.[46] A novel polyether-based GPE *via* copolymerization of DOL and tetrahydrofuran (THF) initiated by $LiPF_6$ (Figure 11a).[46a] These copolymer-based GPEs achieved a high Li^+ transference number of 0.64, benefitting the Li^+ diffusion process and electric potential distribution around the Li metal anode. Besides, an interpenetrating network was constructed *via* the polymerization of DOL and crosslinking of cyanoethyl polyvinyl alcohol (PVA-CN).[46b] The as-prepared GPE exhibited a high ionic conductivity of 3.23×10^{-3} S/cm at 25 °C and a high Li^+ transference number of 0.81. The polyDOL could promote uniform Li deposition and suppress the volume expansion of the Li metal anode. The crosslinked PVA-CN network with polar carbonyl groups could inhibit the solubility and shuttling of polysulfides on the cathode side. To improve the mechanical strength of polyDOL, DOL was *in situ* polymerized in a polydopamine (PDA)-modified PVDF-HFP nanofibrous skeleton (Figure 11b). The polar groups on PDA could form hydrogen bonds with the ether oxygen group and terminal hydroxyl group on polyDOL, benefitting mechanical strength and ionic conductivity of GPE. Meanwhile, the hydrogen bond interaction could prevent the side reaction between the terminal hydroxyl group and Li metal. Therefore, the PDOL@PDA/PVDF-HFP GPE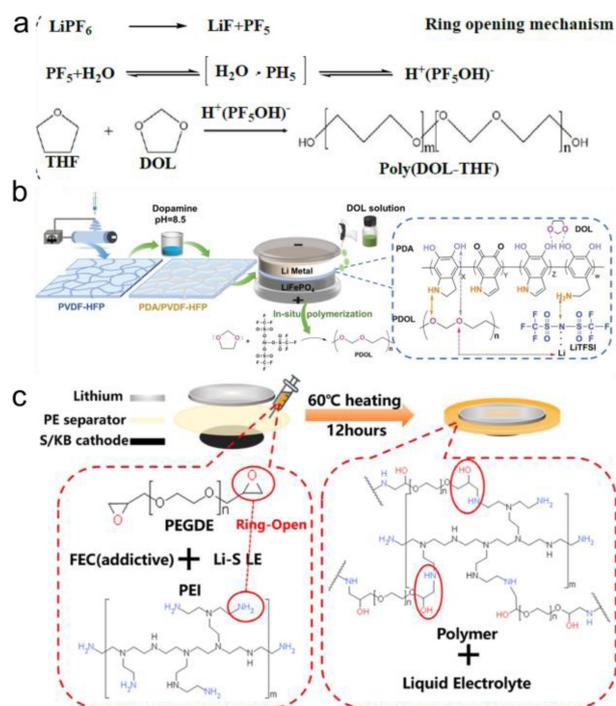 possessed high ionic conductivity of 2.39×10^{-3} S/cm at 25 °C, the wide electrochemical window of 4.57 V *vs.* Li/Li^+, Li^+ transference number of 0.59 and low interface resistance.[46c]

Poly(ethylene glycol)diglycidyl ether (PEGDE) with two cyclic ether units has been used to *in situ* synthesize crosslinked GPEs *via* ring-opening polymerization.[40b,47] A novel GPE was synthesized *via* the ring-opening addition polymerization of polyethyleneimine (PEI) and PEGDE (Figure 11c).[47b] The ether chain in PEGDE and the amino group in PEI could facilitate Li^+ transport for their strong interactions with Li^+. Besides, $-NH-$, $C-N-C$, $-OH$, and $C-O-C$ in the polymer matrix provided Lewis-base sites to constrain polysulfides within the cathode side.[47b]

Various additives have been used to improve the performance of GPEs. Low freezing point solvents can facilitate ion transport at subzero temperatures. A low-temperature operating polyDOL-based GPE was developed with the addition of methyl propionate (MP).[48] MP with the freezing point at −88 °C significantly improved the low-temperature performance of GPEs (e.g., 1.0×10^{-3} S/cm at −30 °C). Flame-retardants are also incorporated to enhance the safety of GPEs. A non-flammable GPE composed of Al_2O_3 and polyDOL showed high safety.[49] The H^+ derived from acid-treated nano Al_2O_3 first attached to lone pair electrons of oxygen atom and initiated the ring-opening polymerization of DOL. The $-OH$ on the surface of acid-treated nano Al_2O_3 could attract $TFSI^-$ anions by Lewis acid-base interaction and facilitate Li^+ transport. Furthermore, owing to the fire-retarding property of Al_2O_3, the as-prepared GPE possessed a high oxygen index of 22.2%.

3.2. Crosslinking of linear ether oligomer

Tetraethylene glycol dimethyl ether (TEGDME, G4) is a common solvent used in Li-air batteries, due to its low viscosity, high reduction resistance, and stability against the nucleophilic attack of superoxide radicals.[41a] However, ether solvent is highly volatile and flammable. By gelation into quasi-solid state GPE, its safety can be enhanced. A new GPE was prepared by directly cross-linking liquid G4 with lithium ethylenediamine (LiEDA) (Figure 12).[41b] The *in situ* formed GPE ensured a good interfacial contact with both cathode and anode. Meanwhile, the electrolyte-derived GPEs avoided contamination from non-electrolytic ions or polymer matrices. The GPE barrier could also
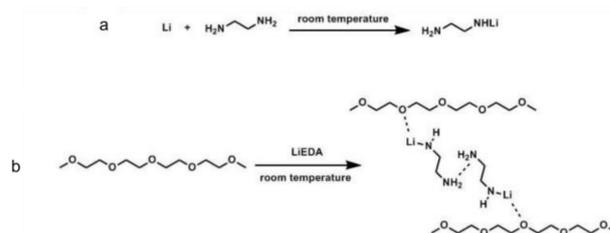

Figure 11. a) Copolymerization mechanism of poly(DOL-co-THF)-based GPE. Reproduced with permission from Ref. [46a]. Copyright (2022) American Chemical Society. b) *In situ* preparation of 3D PDOL@PDA/PVDF-HFP GPE. Reproduced with permission from Ref. [46c]. Copyright (2022) Wiley-VCH. c) Synthesis scheme of the polyethyleneimine (PEI) and poly(ethylene glycol)diglycidyl ether (PEGDE) *via in situ* thermal polymerization. Reproduced with permission from Ref. [47b]. Copyright (2021) American Chemical Society.

Figure 12. Crosslinking reaction mechanism of tetraethylene glycol dimethyl ether (G4) and lithium ethylenediamine (LiEDA). Reproduced with permission from Ref. [41b]. Copyright (2018) John Wiley and Sons.

Batteries & Supercaps

Perspective
doi.org/10.1002/batt.202300057

Chemistry Europe
European Chemical
Societies Publishing

protect the Li metal anode from corrosion by H_2O in the ambient air.

4. Other GPEs

4.1. Poly(ionic liquid)s

In recent years, poly(ionic liquid)s have been developed by incorporating ionic liquid-type monomers into the polymer backbone.[50] Poly(ionic liquid)s inherit the advantages of ionic liquids, such as good ionic conduction, non-flammability, and high electrochemical stability, and also have extra advantages, such as excellent mechanical properties and good processability. Besides, the chemical affinity between the poly(ionic liquid)s and ionic liquids prevent them from phase separation and enhance the safety and performance of ionic liquid-based GPEs.[51]

Poly(ionic liquid)s have high oxidation stability for high voltage cathodes but inferior capability to form a uniform, dense SEI layer on Li anodes. Therefore, combining cyclic carbonate and ionic liquid can simultaneously achieve good compatibility with both electrodes. A novel GPE was *in situ* prepared *via* random copolymerization of a quaternary ammonium salt-based monomer of 2-(methacryloyloxy)-N,N,N-trimethylethanaminium hexafluorophosphate (NPF_6) and a cyclic carbonate-containing monomer of 2-((((2-oxo-1,3-dioxolan4-yl)methoxy)carbonyl)amino)ethyl methacrylate (CUMA) (Figure 13a).[52] By integrating the oxidation stability of NPF_6 and Li anodes compatibility of CUMA, the P(CUMA-NPF_6) GPEs delivered a wide window of 0–5.6 V *vs.* Li/Li$^+$, large Li$^+$ transference number of 0.61, and superior electrode/electrolyte interface compatibility. To improve the safety of GPEs, a fire-retardant GPE was synthesized *via in situ* polymerization of the ionic liquid monomer grafted on SiO_2 nanoparticles in PVDF-HFP porous membranes.[53] The nano-SiO_2 anchored poly(ionic liquid)s constructed ion migration channels to facilitate ion transport. Simultaneously, the silica layer acted as a physical barrier to endow the GPEs with fire safety.

4.2. Cyanoethyl polyvinyl alcohol

Cyanoethyl polyvinyl alcohol (PVA-CN) exhibits high thermodynamic stability and resistance to electrochemical oxidation and has been used to *in situ* prepare GPEs.[54] The cyano resin in PVA-CN was initiated by PF_5 derived from $LiPF_6$ and polymerized into crosslinked GPEs *via* cationic polymerization mechanism (Figure 13b).[54b] The interactions between nitrile groups (—C≡N) and Li$^+$ benefit salt dissolution and dissociation. The *in situ* preparation method significantly reduced the interfacial resistance and benefited the formation of a more stable SEI on the anode.
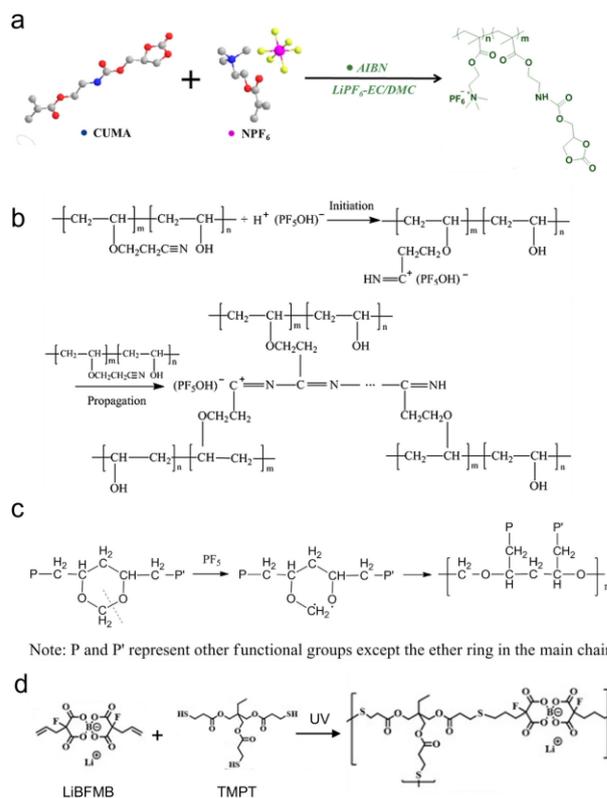

Figure 13. a) Schematic diagram of the polymerization process of the P(CUMA-NPF_6) GPE. Reproduced with permission from Ref. [52]. Copyright (2020) American Chemical Society. b) Polymerization mechanism of PVA-CN in electrolyte solvents. Reproduced with permission from Ref. [54b]. Copyright (2014) Royal Society of Chemistry. c) Schematic representation of the polymerization mechanism of the poly(vinyl formal) (PVFM)-based GPE. Reproduced with permission from Ref. [55]. Copyright (2014) Elsevier. d) Schematic illustration of the *in situ* preparation of a boron-centered fluorinated single-ion conducting polymer electrolyte. Reproduced with permission from Ref. [56]. Copyright (2020) American Chemical Society.

4.3. Poly(vinyl acetal)

Polyvinyl acetal is a suitable polymer matrix for Li batteries because of its high conductivity, unique film-forming properties, and excellent adhesion on many surfaces. The C=O bond in the side chains of polyvinyl acetal can interact with the oxygen atoms of liquid electrolytes and thus exhibit high liquid absorption.[55] A polyvinyl formal (PVFM)-based GPE was *in situ* prepared *via* an initiator-free thermal polymerization method (Figure 13c). PVFM with tri-functional groups, *i.e.*, vinyl formal, vinyl hydroxyl and vinyl acetate, turned into a crosslinked GPE at 60 °C for 6 h, exhibiting high conductivity of 8.82×10^{-3} S/cm at 25 °C and wide electrochemical window of 1.5–5 V *vs.* Li/Li$^+$.

4.4. Single-ion conductor

Single-ion conducting polymer electrolytes are constructed by covalently immobilizing anionic groups onto the polymer backbone, allowing Li$^+$ to move from one anion site to another along the polymer backbone. Therefore, single-ion conducting polymer electrolytes have a high Li$^+$ transference number close

Batteries & Supercaps

Perspective
doi.org/10.1002/batt.202300057

Chemistry
Europe
European Chemical
Societies Publishing

to 1, benefitting a homogeneous ion concentration distribution. A boron-centered fluorinated single-ion conducting polymer electrolyte was synthesized *via* UV-initiated polymerization between trimethylolpropane tris(3-mercapto propionate) and lithium bis(fluoroallyl)malonato borate (LiBFMB) (Figure 13d).[56] Owing to the high efficiency of thiol-ene click reactions, BFMB⁻ anions were all anchored on the polymer skeleton and lost mobility. The noncoordinating sp^3 boron center showed weak coordination with Li^+ and benefitted Li^+ transport. Meanwhile, the strong electron withdrawing nature of fluorine could increase the anodic stability. The as-prepared single-ion conducting polymer electrolytes achieved a high Li^+ transference number of 0.93 and an ionic conductivity of 2×10^{-4} S/cm at 35 °C, mainly contributed by Li^+.

In this Section, we have introduced the synthesis and performance of various *in situ* GPEs based on polymer matrix, mainly including polyester and polyether. Polyester-based GPEs are usually synthesized *in situ* by free radical polymerization mechanism. They contain carbonyl groups and show strong interactions with the oxygen groups in carbonate solvents, thus exhibiting high electrolyte absorption and excellent ionic conductivity. Polyether-based GPEs can be synthesized *via* cationic polymerization mechanism under mild external conditions, such as at room-temperature and without initiators, which is promising to accommodate industrial production. Besides, other novel types of *in situ* GPEs was also introduced, such as poly(ionic liquid)s, cyanoethyl polyvinyl alcohol, poly(vinyl acetal), single-ion conductor. The compositon and performance of different *in situ* GPEs were summarized in Table 1. We also summarized the novel structural and functional designs of *in situ* GPEs. *In situ* synthesized GPEs have the advantages of high ionic conductivity, intimate interfacial contact with electrodes, and enhanced safety, which are expected to be widely used in high-performance quasi-solid-state Li batteries.

5. Applications

With the development of electric vehicles and wearable electronics, Li batteries are developing towards high energy density and high safety. However, Li batteries using liquid electrolytes are faced with unsatisfactory performance and safety concerns. The emerging *in situ* GPEs can prevent electrolyte leakage, suppress dendrite growth, prevent polysulfide shutting, and inhibit O_2 crossover, thereby greatly enhancing the battery performance. This section summarized the applications of *in situ* GPEs in different Li batteries, such as Li-ion battery, Li-metal battery, Li-sulfur battery and Li-air battery.

5.1. Li-ion battery

Li-ion batteries have the advantages of high energy density and long cycle life. After commercialization for over 30 years, Li-ion batteries have become the preferred energy source for portable electronics, electric vehicles, and large-scale energy storage systems.[21] However, intrinsically flammable liquid electrolytes are challenged with leakage, combustion, and even explosion.[38a] By encapsulating flammable organic solvents in polymer matrix, GPE prevents leakage and exhibits high ionic conductivity close to liquid electrolyte.[54b] For *in situ* GPE, gel precursor with low viscosity can fully permeate porous electrodes and form compact electrode/electrolyte interface, achieving high utilization of active materials.[18b] By forming SEI layer before gelation, the interfacial resistance could be further reduced (Figure 14a). Compared with *ex situ* GPE, LIBs with *in situ* GPE exhibited improved performance in terms of capacity retention, Coulombic efficiency, and cycle life.[40b,54b]
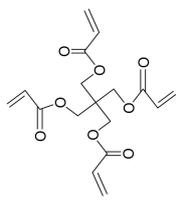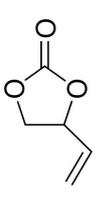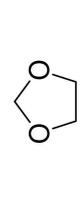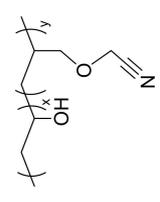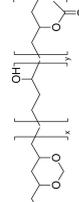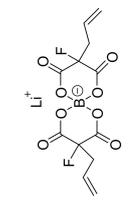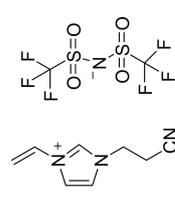
Combining GPE with high performance electrodes can further increase the energy density of LIBs. Si electrodes have a high specific capacity of 4200 mAh/g but suffer from significant volume change during lithiation and delithiation. *In situ* formed PETEA-based GPE with the robust network could maintain a tight interface with the Si anode and suppress its volume change during lithiation and delithiation (Figure 14b). The as-fabricated Si-C/NCA batteries still kept 81.2% capacity after 200 cycles at 5C.[14b] High-voltage cathodes, such as olivine type $LiCoPO_4$, spinel $LiNi_{0.5}Mn_{1.5}O_4$, layered $LiCoO_2$, and $Li-Ni_xCo_yMn_zO_2$, have also been used in high-energy-density Li-ion batteries.[57] However, conventional carbonate-based liquid electrolytes decompose at 4.5 V *vs.* Li/Li^+ and cannot accommodate 4.6 V $LiNi_{0.5}Mn_{1.5}O_4$ cathode.[16] Electrolyte decomposition may further trigger the dissolution of transition metal on the cathode. The *in situ* crosslinked poly(acrylic anhydride-2-methyl-acrylic acid-2-oxirane-ethyl ester-methyl methacrylate) (PAMM) GPE showed a broad voltage window (above 5 V) to avoid decomposition and served as a physical barrier to suppress transition metal dissolution (Figure 14c). $Li_4Ti_5O_{12}/LiNi_{0.5}Mn_{1.5}O_4$ cell showed improved Coulombic efficiency of 96% after 100 cycles at 0.1 C (Figure 14d).[27]

5.2. Li-metal battery

Traditional Li-ion batteries with graphene anodes are approaching the theoretical specific energy of 300 Wh/kg, which still cannot fulfill the emerging needs of electric vehicles, 5G telecommunication, and smart grids.[42a] Li metal anode has the ultra-high theoretical specific capacity (3860 mAh/g), the lowest redox potential (−3.04 V *vs.* SHE), and lightweight (0.534 g/cm), which thus is considered as an ideal anode for high-energy-density battery.[58] Unfortunately, Li metal anode suffers from the long-standing dendrite problem, which causes poor cycling performance and severe safety hazards. Therefore, Li-metal batteries have lagged behind Li-ion batteries in the commercialization process since the 1980s.[43b]

In Li-metal batteries, Li metal anode is highly reactive and spontaneously react with organic electrolyte at the electrode/electrolyte interface to form a solid electrolyte layer (SEI), which can prevent further side reactions. However, the SEI layer cannot accommodate Li volume change in repeated Li plating/striping with constantly generated cracks.[59] Li ions accumulate around these defects and deposit in a dendritic manner.[60]

Table 1. Composition and performance of *in situ* GPEs with different polymer hosts.

No.	Liquid electrolyte	Monomer	Preparation	Performance	Ref.
1	1 M LiTFSI in DOL:DME (1:1, v/v) with 1 wt% LiNO$_3$		AIBN, 75 °C for 2 h	$\sigma = 11.3$ mS/cm at 25 °C	[14a]
2	0.15 M LiBOB + 1 M LiTFSI in VEC		AIBN, 70 °C for 5 h	$\sigma = 6.9$ mS/cm at 25 °C $t_{Li+} = 0.512$ 5.3 V vs. Li/Li$^+$	[16]
3	2 M LiPF$_6$ + 1 M LiTFSI in DOL:DME (1:1, v/v)		room temperature	$\sigma = 3.8$ mS/cm at 25 °C	[40a]
4	1 M LiPF$_6$ in EC:EMC (1:2, v/v)		60 °C, one day	$\sigma = 8.63$ mS/cm at 23 °C $t_{Li+} = 0.84$	[54a]
5	1 M LiPF$_6$ in EC:DMC (3:7, v/v)		60 °C for 6 h	$\sigma = 8.82$ mS/cm at 25 °C 1.5–5 V vs. Li/Li$^+$	[55]
6	1 M LiBFMB in PC:EC:FEC (6:3:1,v/v/v)		DMPA, UV-vis light for 15 min	$\sigma = 0.2$ mS/cm at 35 °C $t_{Li+} = 0.93$	[56]
7	1 M LiPF$_6$ in EC:DMC:EMC (1:1:1, v/v/v)		60 °C for 1 h	$\sigma = 4.97$ mS/cm at 25 °C $t_{Li+} = 0.69$	[57]

Solvent – DOL: 1,3-dioxane; DME: 1,2-dimethoxyethane; VEC: 4-vinyl-1,3-dioxolan-2-one; EC: ethylene carbonate; EMC: ethyl methyl carbonate; PC: propylene carbonate; FEC: fluoroethylene carbonate; DMC: dimethyl carbonate. Salt – LiTFSI: lithium bis(trifluoromethanesulfonyl)imide; LiNO$_3$: lithium nitrate; LiDBOB: lithium bis(oxalate)borate; LiPF$_6$: lithium hexafluorophosphate; LiBFMB: lithium bis(fluoroallyl)malonato borate. σ: ionic conductivity. t_{Li+}: Li$^+$ transference number.
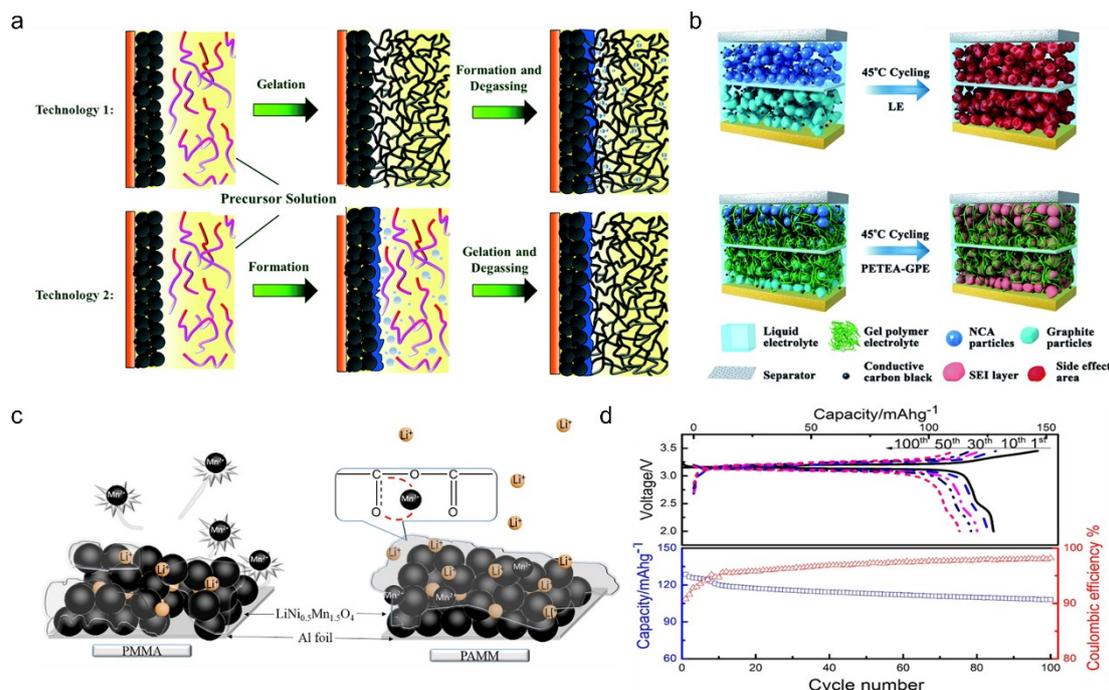
Figure 14. a) Schematic illustration for the gelation and formation of PVA-CN based polymer LIBs with different formation. Reproduced with permission from Ref. [54b]. Copyright (2014) Royal Society of Chemistry. b) Schematic illustration of Li-ion batteries with liquid electrolyte and *in situ* PETEA-GPE during cycling. Reproduced with permission from Ref. [14b]. Copyright (2017) Royal Society of Chemistry. c) Schematic of suppressed Mn^{2+} dissolution by PAMM GPE. d) Cycling performance of $Li_4Ti_5O_{12}/LiNi_{0.5}Mn_{1.5}O_4$ cell. Reproduced with permission from Ref. [27]. Copyright (2017) American Chemical Society.

Eventually, uncontrollable dendrites will pierce the separator, inducing short circuit and thermal runaway of batteries. Therefore, stabilizing the interface between Li metal and electrolyte is vital for the application of Li-metal batteries.

In situ GPEs can form intimate interfacial contact with Li metal and homogenize Li^+ flux on the anode surface. Combining strong interface adhesion and elastic mechanical property, *in situ* GPE can maintain intimate interface with Li metal anode during the charge-discharge process (Figure 15a).[19a] As shown in scanning electron microscope (SEM) images, the Li electrode showed a rough surface with dead Li after cycling in the liquid electrolyte (Figure 15b). In contrast, the Li electrode maintained a smooth and compact surface in GPE (Figure 15c). Li/NCM622 showed a Coulombic efficiency close to 100 % and achieved 81 % capacity retention under 2C after 400 cycles. Increasing the mechanical strength of *in situ* GPE also helps to suppress Li dendrites. Recently, a self-enhancing GPE *via* hydrogen bond interaction between polyDOL and polydopamine was designed (Figure 15d).[46c] The overpotential of Li symmetric cells was less than 25 mV over 250 hours, showing excellent suppression of Li dendrites. The GPE-based Li/LFP batteries showed extraordinary cyclic stability over 800 cycles at a high current density of 2C (Figure 15e). Strengthening the SEI layer could also suppress the dendrite growth. By adding classical electrolyte additives in GPEs, like fluoroethylene carbonate (FEC), a robust fluorinated SEI layer was constructed to effectively reduce dendrite growth.[59] Poly(ionic liquid)s[52] and dual-salt GPE[61] were also developed to stabilize Li metal anode.

For Li-metal batteries under charging, rapid plating and limited diffusion of Li^+ ions accelerate Li^+ depletion at the anode surface. Meanwhile, excessive Li^+ ions accumulate on the cathode and a stronger electric field is built in the battery. Under high electric field, Li^+ is preferentially deposited on the surface protrusions to form dendrites. Therefore, reducing Li^+ concentration polarization on the Li anode surface can also suppress dendrite growth.[62] By anchoring anions on the polymer backbone, single-ion conducting polymer electrolytes with a high Li^+ transference number can effectively alleviate concentration polarization.[63] For example, a Li-containing boron-centered fluorinated single-ion conducting GPE achieved an ionic conductivity of 2×10^{-4} S/cm at 35 °C and high Li^+ transference number of 0.93.[56] For GPE, only a slight variation appeared after 120 s, while steep Li^+ concentration gradients were observed in liquid electrolytes (Figure 14f and 14g). Integrating the GPE with electrodes *in situ*, Li/LFP cells showed a promising average Coulombic efficiency of 99.95 % over 200 cycles, indicating the long-term stability of Li-metal batteries with the single-ion conducting GPE (Figure 14h).

Although many approaches have been studied to avoid Li dendrites, nonflammable GPEs are also necessary for Li metal batteries to eliminate high security risks.[64] Adding fire-retardant additives to *in situ* GPE showed enhanced thermal stability, enabling the as-prepared pouch cells with excellent abusive resistance. Meanwhile, the fire-retardants showed good compatibility with Li metal anode, and the Li/NCM811 cells yet stably cycled over 200 times at 1C, with a capacity retention
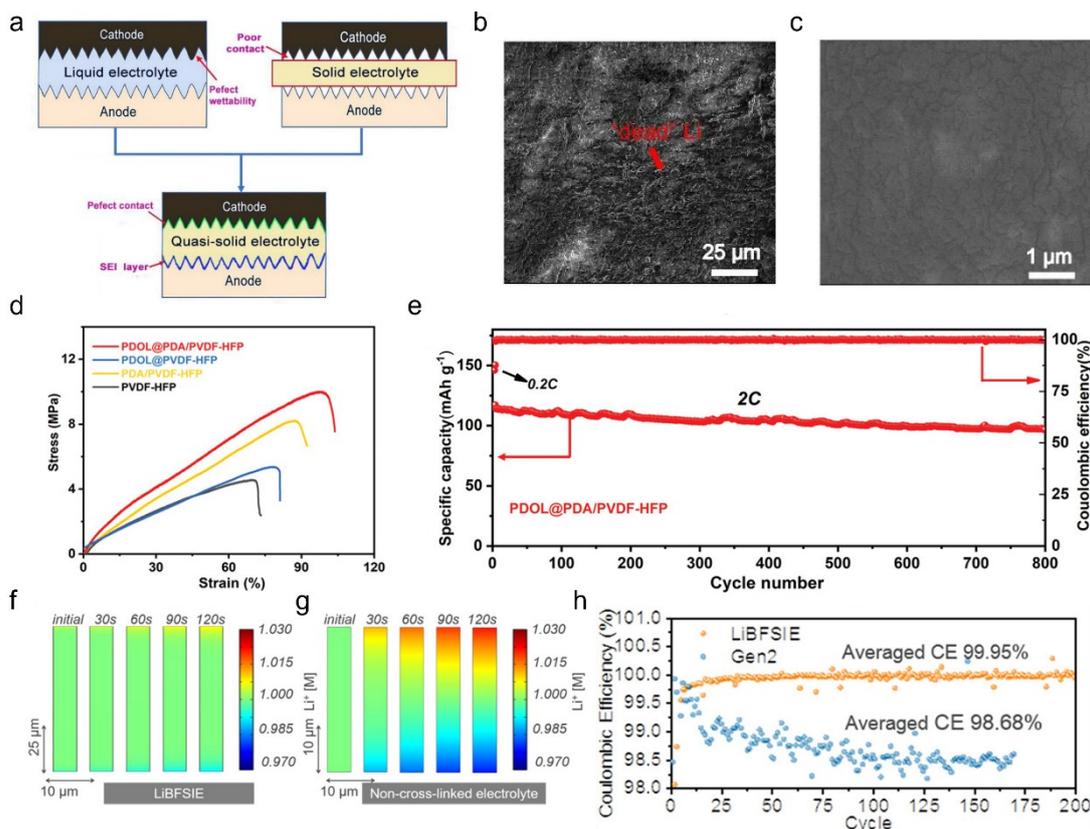
Figure 15. a) Illustration of interfaces with liquid electrolyte, solid electrolyte, and *in situ* GPE, respectively. b, c) Surface morphology of Li anode after cycling in liquid electrolyte and *in situ* GPE, respectively. Reproduced with permission from Ref. [19a]. Copyright (2020) Elsevier. d) Stress-strain curves of PVDF-HFP, PDA/PVDF-HFP membranes, PDOL@PVDF-HFP and PDOL@PDA/PVDF-HFP GPEs, respectively. e) Cycling performance of PDOL@PDA/PVDF-HFP GPE. Reproduced with permission from Ref. [46c]. Copyright (2021) The Authors. Published by Wiley-VCH. f, g) Simulation results of Li$^+$ concentration distribution in single-ion conducting GPE and liquid electrolyte, respectively. h) Coulombic efficiency of Li/LFP cell with GPE (orange) and liquid electrolyte (blue). Reproduced with permission from Ref. [56]. Copyright (2020) American Chemical Society.

rate of 85.3%.[65] Besides, employing non-flammable poly(ionic liquid)s can also improve battery safety.[53,66]

5.3. Li-sulfur battery

Li-sulfur batteries hold potential for next-generation battery systems due to their high theoretical energy density (2600 Wh/kg), over 10 times higher than traditional Li-ion batteries. Sulfur cathode also takes advantage of natural abundance, non-toxicity, low material cost, and environmental benignity.[47b] However, Li-sulfur batteries face low sulfur utilization, poor rate capability, and short cycle life, mainly attributed to the shuttle effect of polysulfide. During the discharge process, sulfur is reduced to polysulfide intermediate, which dissolves into a liquid electrolyte, diffuses to the anode and further reacts with Li metal, causing active materials loss.

Replacing liquid electrolytes with *in situ* GPEs can efficiently alleviate the shuttle effect of polysulfides (Figure 16a).[14c,26] By tailoring crosslinking structure[67] and polar functional groups,[25] GPEs could barrier polysulfide diffusion and capture the polar sulfur discharge products. Such Li-sulfur battery exhibited low interfacial resistance, high rate capacity (601.2 mAh/g at 1C) and improved capacity retention than those with liquid electro-

lytes (Figure 16b).[14a] Self-discharge of Li-sulfur batteries was also inhibited by the use of crosslinked *in situ* GPE. Both experimental results and first-principal calculations revealed that acrylate-based hierarchical electrolytes (AHE) could effectively reduce polysulfide diffusion. No apparent color change was observed in the AHE cell during the 2 hour aging test. (Figure 16c).[68]

5.4. Li-air battery

Li-air batteries, consisting of a Li metal anode, Li$^+$ conducting electrolyte, and porous air cathode, have an ultra-high theoretical energy density of 3500 Wh/kg.[69] However, Li-air batteries are limited by inherent semi-open structure. Liquid electrolytes easily vaporize and release flammable gas to ambient air.[70] Meanwhile, O$_2$ and H$_2$O in the air can penetrate liquid electrolytes and corrode the Li metal anode.[71] By encapsulating liquid electrolytes in polymer networks and blocking air crossover, *in situ* GPEs can suppress volatilization and leakage of liquid electrolytes and protect the Li anode from corrosion. *In situ* formed gel enhanced the cycling performance of Li-air batteries to 1175 hours (Figure 17a).[41b] With crosslinked GPEs, a Li-air battery delivered a specific
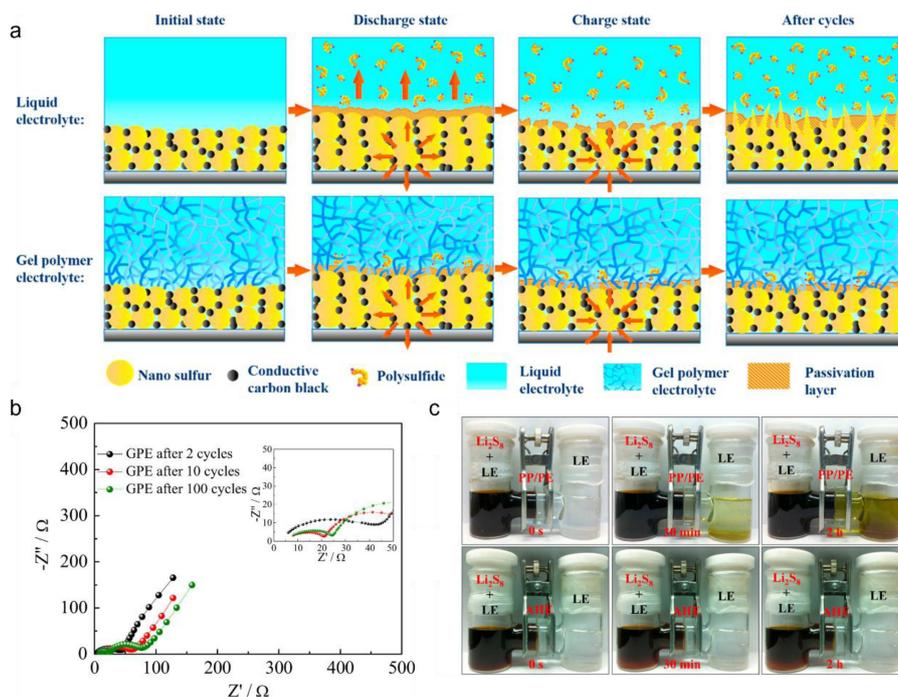
Batteries & Supercaps

Perspective
doi.org/10.1002/batt.202300057

Chemistry Europe
European Chemical
Societies Publishing

Figure 16. a) Schematic of polysulfides immobilized by PETEA-based GPE. b) Electrochemical impedance spectroscopy plots of Li/GPE/S cell. Reproduced with permission from Ref. [14a]. Copyright (2016) Elsevier. c) Durability test of commercial separator and acrylate-based hierarchical electrolytes (AHE) between polysulfides and liquid electrolyte. Reproduced with permission from Ref. [68]. Copyright (2016) Elsevier.
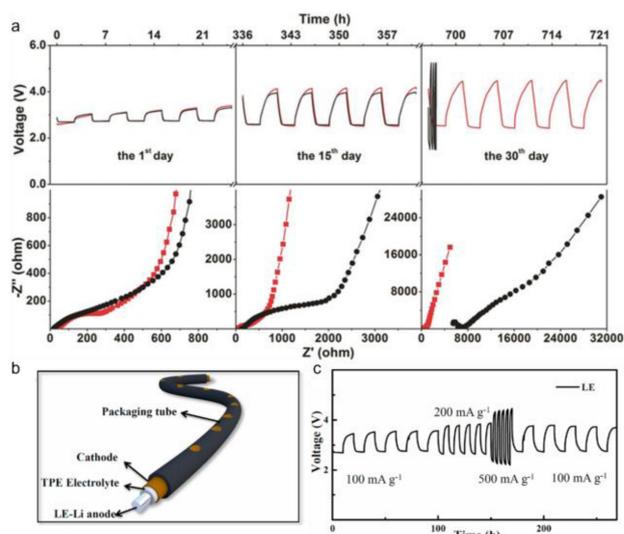

Figure 17. a) The storage performance of coin type Li-air batteries by using G4-based GPE (red) and liquid electrolyte (black) in ambient air, respectively. Reproduced with permission from Ref. [41b]. Copyright (2018) Wiley-VCH. b) Schematic of flexible fiber Li-O$_2$ battery using tetraglyme-based polymer electrolyte (TPE). c) Rate performance of the flexible Li-CO$_2$ with TPE GPEs. Reproduced with permission from Ref. [41c]. Copyright (2021) Elsevier.

capacity of 3898 mAh/g.[69] *In situ* GPE was also applied in Li-CO$_2$ batteries (Figure 17b). The voltage evolution of flexible Li-CO$_2$ battery was very stable at the current density from 100 to 500 mA/g (Figure 17c). The reported cell could steadily run for 104 cycles with a small overpotential, attributed to the resistance of GPE to CO$_2$ permeation.[41c]

6. Conclusions and Perspectives

In situ synthesized GPEs have been intensively studied to accelerate the industrial-scale production of safe, high energy, and flexible lithium batteries, which simplify the preparation and form integrated electrode/electrolyte interface. In this perspective, the recent progress of *in situ* GPEs was summarized, including synthesis, performance and applications. Based on polymer host, the synthesis conditions and design strategies of *in situ* GPEs have been systematically summarized. Besides, the electrochemical and mechanical properties of *in situ* GPEs were discussed. Finally, the applications of *in situ* GPEs in different Li batteries have been summarized. Despite great progresses of *in situ* GPEs in Li batteries, there are still some challenges to be solved.

1) For *in situ* synthesis of GPEs, limited studies cover *in situ* polymerization process and mechanism. The currently reported polymerization methods generally require high temperature and nonelectrolyte initiators, which may affect battery performance. Besides, the polymerization degree and uniformity are key to the electrochemical and mechanical properties of *in situ* GPEs. The remaining monomers may decompose at the electrode surface, increase interfacial resistance and degrade battery performance. Therefore, new polymerization methods with mild reaction conditions and high conversion need to be investigated.

2) For the performance of *in situ* GPEs, they still cannot satisfy the practical applications, such as insufficient transport capacity at low temperature or high rate, poor oxidative stability towards high-voltage cathode and compromised

safety. Therefore, molecular-level (e.g., copolymerization, blending, composite and crosslinking) and functional (e.g., flame-retardant, self-healing, or wide-temperature working capabilities) design should also be developed to satisfy different applications.

3) For the applications of *in situ* GPEs, the fundamental studies of solid-state Li batteries using *in situ* GPEs is sufficient. Because polymer precursor is injected to the cell before battery assembly, it remains a challenge to monitor electrode/electrolyte interface during *in situ* polymerization and charge-discharge process. Therefore, advanced characterization techniques and theoretical computations are urgently needed to provide theoretical guidance in interface modification and performance improvement for lithium batteries with *in situ* GPEs.

Although *in situ* GPEs have demonstrated great potential in achieving high-performance solid-state Li batteries, there are still several challenges in basic research and practical applications, which require interdisciplinary cooperation from polymer chemistry, electrochemistry, interface science and engineering. We believe that *in situ* polymerization of solid-state Li batteries GPEs will approach practical applications after extensive scientific research.

Acknowledgements

Conflict of Interest

The authors declare no conflict of interest.

[1] J. M. Tarascon, M. Armand, *Nature* **2001**, *414*, 359–367.
[2] J. Janek, W. G. Zeier, *Nat. Energy* **2016**, *1*, 16141.
[3] M. D. Tikekar, S. Choudhury, Z. Tu, L. A. Archer, *Nat. Energy* **2016**, *1*, 16114.
[4] G. Feuillade, P. Perche, *J. Appl. Electrochem.* **1975**, *5*, 63–69.
[5] F. Baskoro, H. Q. Wong, H.-J. Yen, *ACS Appl. Energ. Mater.* **2019**, *2*, 3937–3971.
[6] Q. Zhao, X. Liu, S. Stalin, K. Khan, L. A. Archer, *Nat. Energy* **2019**, *4*, 365–373.
[7] Y.-G. Cho, C. Hwang, D. S. Cheong, Y.-S. Kim, H.-K. Song, *Adv. Mater.* **2019**, *31*, 1804909.
[8] A. Manthiram, X. Yu, S. Wang, *Nat. Rev. Mater.* **2017**, *2*, 16103.
[9] T. Liu, J. Zhang, W. Han, J. Zhang, G. Ding, S. Dong, G. Cui, *J. Electrochem. Soc.* **2020**, *167*, 070527.
[10] C. Ma, W. Cui, X. Liu, Y. Ding, Y. Wang, *InfoMat* **2022**, *4*, e12232.
[11] a) A. Hosseinioun, E. Paillard, *J. Membr. Sci.* **2020**, *594*, 117456; b) J. L. Wang, F. Y. Liu, Z. Y. Huang, M. R. Wang, Q. Y. Wang, B. Hong, S. M. Li, Z. Zhang, Y. Q. Lai, Y. X. Liu, *Mater. Lett.* **2022**, *324*, 132744; c) Q. C. Wang, X. Y. Ding, J. B. Li, H. B. Jin, H. C. Gao, *Chem. Eng. J.* **2022**, *448*,137740.
[12] S. P. Wu, H. P. Zheng, N. Zhang, W. Z. Cheng, H. Z. Liu, H. N. Duan, *J. Power Sources* **2022**, *542*, 231782.
[13] W. J. Zhang, S. L. Li, Y. R. Zhang, X. H. Wang, J. D. Liu, Y. H. Zheng, *Sci. China Technol. Sci.* **2022**, *65*, 2369–2379.
[14] a) M. Liu, D. Zhou, Y. B. He, Y. Z. Fu, X. Y. Qin, C. Miao, H. D. Du, B. H. Li, Q. H. Yang, Z. Q. Lin, T. S. Zhao, F. Y. Kang, *Nano Energy* **2016**, *22*, 278–289; b) X. L. Li, K. Qian, Y. B. He, C. Liu, D. C. An, Y. Y. Li, D. Zhou, Z. Q. Lin, B. H. Li, Q. H. Yang, F. Y. Kang, *J. Mater. Chem. A* **2017**, *5*, 18888–18895; c) M. Liu, D. Zhou, H. R. Jiang, Y. X. Ren, F. Y. Kang, T. S. Zhao, *Nano Energy* **2016**, *28*, 97–105.
[15] Y. M. Jin, X. Zong, X. B. Zhang, Z. G. Jia, H. J. Xie, Y. P. Xiong, *Energy Storage Mater.* **2022**, *49*, 433–444.
[16] Q. J. Zhou, C. K. Fu, R. L. Li, X. Y. Zhang, B. X. Xie, Y. Z. Gao, G. P. Yin, P. J. Zuo, *Chem. Eng. J.* **2022**, *437*, 135419.
[17] Y. Zhang, J. R. Wang, C. Zhang, Z. G. Xue, *Mater. Today Energy* **2022**, *29*, 101107.
[18] a) L. X. Fu, L. Y. Shi, Z. Y. Wang, J. F. Zhu, Y. Zhao, S. Yuan, *Res. Chem. Intermed.* **2019**, *45*, 4959–4973; b) S. Z. Zhang, X. H. Xia, D. Xie, R. C. Xu, Y. J. Xu, Y. Xia, J. B. Wu, Z. J. Yao, X. L. Wang, J. P. Tu, *J. Power Sources* **2019**, *409*, 31–37; c) D. S. Shao, X. Y. Wang, X. L. Li, K. L. Luo, L. Yang, L. Liu, H. Liu, *J. Solid State Electrochem.* **2019**, *23*, 2785–2792; d) Z. N. Man, H. Tian, X. B. Zhu, Y. Wang, Y. G. Wu, X. Y. Wen, Z. Lu, *J. Electrochem. Soc.* **2022**, *169*, 060507.
[19] a) Z. Li, X. Y. Zhou, X. Guo, *Energy Storage Mater.* **2020**, *29*, 149–155; b) C. H. Tsao, Y. T. Lin, S. Y. Hsu, S. Okada, D. N. Kuo, S. S. Hou, P. L. Kuo, *Electrochim. Acta* **2020**, *361*, 137076.
[20] Q. Y. Wang, X. Q. Xu, B. Hong, M. H. Bai, J. Li, Z. A. Zhang, Y. Q. Lai, *Energy Environ. Sci.* **2022**, *0*, 1–12.
[21] B. Jeong, D. A. Lim, H. M. Kim, J. Y. Kim, D. W. Kim, *J. Electrochem. Soc.* **2021**, *168*, 100538.
[22] Y. Ma, Q. F. Sun, Z. Y. Wang, S. Wang, Y. Zhou, D. W. Song, H. Z. Zhang, X. X. Shi, C. L. Li, L. Q. Zhang, L. Y. Zhu, *J. Mater. Chem. A* **2021**, *9*, 3597–3604.
[23] K. Dai, C. Ma, Y. M. Feng, L. J. Zhou, G. C. Kuang, Y. Zhang, Y. Q. Lai, X. W. Cui, W. F. Wei, *J. Mater. Chem. A* **2019**, *7*, 18547–18557.
[24] J. Y. Zheng, X. Li, Y. J. Yu, X. M. Zhen, Y. Y. Song, X. M. Feng, Y. F. Zhao, *J. Solid State Electrochem.* **2014**, *18*, 2013–2018.
[25] J. Y. Liang, R. M. Tao, J. Tu, C. Guo, K. Du, R. Guo, W. Zhang, X. L. Liu, P. M. Guo, D. Y. Wang, S. Dai, X. G. Sun, *J. Mater. Chem. A* **2022**, *10*, 12563–12574.
[26] H. P. Du, S. Z. Li, H. T. Qu, B. Y. Lu, X. G. Wang, J. C. Chai, H. R. Zhang, J. Ma, Z. H. Zhang, G. L. Cui, *J. Membr. Sci.* **2018**, *550*, 399–406.
[27] Y. Ma, J. Ma, J. C. Chai, Z. H. Liu, G. L. Ding, G. J. Xu, H. S. Liu, B. B. Chen, X. H. Zhou, G. L. Cui, L. Q. Chen, *ACS Appl. Mater. Interfaces* **2017**, *9*, 41462–41472.
[28] D. Zhou, R. L. Liu, Y. B. He, F. Y. Li, M. Liu, B. H. Li, Q. H. Yang, Q. Cai, F. Y. Kang, *Adv. Energy Mater.* **2016**, *6*, 1502214.
[29] J. H. Ahn, T. S. You, S. M. Lee, D. Esken, D. Dehe, Y. C. Huang, D. W. Kim, *J. Power Sources* **2020**, *472*, 228519.
[30] a) Q. S. Sun, X. Chen, J. Xie, X. W. Xu, J. Tu, P. Zhang, X. B. Zhao, *RSC Adv.* **2019**, *9*, 42183–42193; b) D. Cai, S. Z. Zhang, M. Su, Z. P. Ma, J. Q. Zhu, Y. Zhong, X. M. Luo, X. L. Wang, X. H. Xia, C. D. Gu, J. P. Tu, *J. Membr. Sci.* **2022**, *661*, 120907.
[31] a) D. Cai, X. H. Qi, J. Y. Xiang, X. Z. Wu, Z. X. Li, X. M. Luo, X. L. Wang, X. H. Xia, C. D. Gu, J. P. Tu, *Chem. Eng. J.* **2022**, *435*, 135030; b) Y. Zhou, Y. Tian, W. Wang, Y. Zhou, *Electrochim. Acta* **2022**, *434*, 141353; c) M. Liu, W. H. Xie, B. Li, Y. B. Wang, G. Q. Li, S. T. Zhang, Y. H. Wen, J. Y. Qiu, J. H. Chen, P. C. Zhao, *ACS Appl. Mater. Interfaces* **2022**, *14*, 43116–43126; d) Z. J. Bi, W. L. Huang, S. Mu, W. H. Sun, N. Zhao, X. X. Guo, *Nano Energy* **2021**, *90*, 106498.
[32] a) Z. C. Shen, J. W. Zhong, S. Y. Jiang, W. H. Xie, S. Y. Zhan, L. Y. Zeng, K. J. Lin, H. L. Hu, G. D. Lin, Y. H. Lin, S. H. Sun, Z. C. Shi, *ACS Appl. Mater. Interfaces* **2022**, *14*, 41022–41036; b) Q. J. Wang, P. Zhang, W. Q. Zhu, D. Zhang, Z. J. Li, H. Wang, H. L. Sun, B. Wang, L. Z. Fan, *J. Materiomics* **2022**, *8*, 1048–1057; c) X. L. Zhang, S. Y. Zhao, W. Fan, J. N. Wang, C. J. Li, *Electrochim. Acta* **2019**, *301*, 304–311.
[33] a) M. Liu, Y. Wang, M. Li, G. Q. Li, B. Li, S. T. Zhang, H. Ming, J. Y. Qiu, J. H. Chen, P. C. Zhao, *Electrochim. Acta* **2020**, *354*, 136622; b) M. Liu, S. T. Zhang, G. Q. Li, C. Wang, B. Li, M. Li, Y. Wang, H. Ming, Y. H. Wen, J. Y. Qiu, J. H. Chen, P. C. Zhao, *J. Power Sources* **2021**, *484*, 229235.
[34] a) C. Liao, X. G. Sun, S. Dai, *Electrochim. Acta* **2013**, *87*, 889–894; b) B. Y. Huang, Y. D. Zhang, M. M. Que, Y. B. Xiao, Y. Q. Jiang, K. Yuan, Y. W. Chen, *RSC Adv.* **2017**, *7*, 54391–54398; c) Y. S. Yun, J. A. Choi, D. W. Kim, *Macromol. Res.* **2013**, *21*, 49–54.
[35] a) C. Gerbaldi, J. R. Nair, S. Ferrari, A. Chiappone, G. Meligrana, S. Zanarini, P. Mustarelli, N. Penazzi, R. Bongiovanni, *J. Membr. Sci.* **2012**, *423*, 459–467; b) Q. J. Wang, P. Zhang, B. Wang, L. Z. Fan, *Electrochim. Acta* **2021**, *370*, 137706.

Batteries & Supercaps

Perspective
doi.org/10.1002/batt.202300057

**Chemistry
Europe**

European Chemical
Societies Publishing

[36] Y. Xu, X. A. Jiang, Z. E. Liu, Z. J. Chen, S. G. Zhang, Y. Zhang, *J. Power Sources* **2022**, *546*, 231952.

[37] a) G. D. Zhou, X. D. Lin, J. P. Liu, J. Yu, J. X. Wu, H. M. Law, Z. Wang, F. Ciucci, *Energy Storage Mater.* **2021**, *34*, 629–639; b) J. H. Chen, Z. Yang, G. H. Liu, C. Li, J. S. Yi, M. Fan, H. P. Tan, Z. H. Lu, C. L. Yang, *Energy Storage Mater.* **2020**, *25*, 305–312; c) Z. Y. Wen, Z. K. Zhao, T. Zhang, Y. S. Wang, J. X. Zhang, Z. Y. Sun, L. Li, Y. J. Li, F. Wu, R. J. Chen, *J. Mater. Chem. A* **2022**, *10*, 21905–21911.

[38] a) X. W. Mu, X. J. Li, C. Liao, H. Yu, H. Yin, B. Yu, L. F. Han, L. K. Chen, Y. C. Kan, L. Song, Y. Hu, *Adv. Funct. Mater.* **2022**, *32*, 2203006; b) J. Y. Zheng, Y. W. Yang, X. M. Feng, X. Li, X. M. Zhen, W. H. Chen, Y. F. Zhao, *React. Funct. Polym.* **2020**, *149*, 104535; c) J. R. Wu, X. S. Wang, Q. Liu, S. W. Wang, D. Zhou, F. Y. Kang, D. Shanmukaraj, M. Armand, T. Rojo, B. H. Li, G. X. Wang, *Nat. Commun.* **2021**, *12*, 5746; d) H. P. Li, Y. X. Kuai, J. Yang, S. l. Hirano, Y. L. Nuli, J. L. Wang, *J. Energy Chem.* **2022**, *65*, 616–622.

[39] a) P. Jaumaux, Q. Liu, D. Zhou, X. F. Xu, T. Y. Wang, Y. Z. Wang, F. Y. Kang, B. H. Li, G. X. Wang, *Angew. Chem. Int. Ed.* **2020**, *59*, 9134–9142; *Angew. Chem.* **2020**, *132*, 9219–9227; b) Z. Li, J. L. Fu, S. Zheng, D. G. Li, X. Guo, *Small* **2022**, *18*, 2200891.

[40] a) F. Q. Liu, W. P. Wang, Y. X. Yin, S. F. Zhang, J. L. Shi, L. Wang, X. D. Zhang, Y. Zheng, J. J. Zhou, L. Li, Y. G. Guo, *Sci. Adv.* **2018**, *4*, eaat5383; b) Y. W. Lee, W. K. Shin, D. W. Kim, *Solid State Ionics* **2014**, *255*, 6–12.

[41] a) J. M. Xu, C. Ma, C. Y. Chang, X. F. Lei, Y. W. Fu, J. Wang, X. Z. Liu, Y. Ding, *ACS Appl. Mater. Interfaces* **2021**, *13*, 38179–38187; b) X. F. Lei, X. Z. Liu, W. Q. Ma, Z. Cao, Y. G. Wang, Y. Ding, *Angew. Chem. Int. Ed.* **2018**, *57*, 16131–16135; *Angew. Chem.* **2018**, *130*, 16363–16367; c) S. S. Zhang, X. Q. Liu, Y. Y. Feng, D. Wang, H. X. Yin, Z. Z. Chi, L. Li, J. Liu, S. X. Li, J. F. Huang, Z. Y. Guo, L. Wang, *J. Power Sources* **2021**, *506*, 230226.

[42] a) Q. Liu, B. Y. Cai, S. Li, Q. P. Yu, F. Z. Lv, F. Y. Kang, Q. Wang, B. H. Li, *J. Mater. Chem. A* **2020**, *8*, 7197–7204; b) Y. Chen, F. Huo, S. M. Chen, W. B. Cai, S. J. Zhang, *Adv. Funct. Mater.* **2021**, *31*, 2102347.

[43] a) J. P. Zheng, W. D. Zhang, C. Y. Huang, Z. Y. Shen, X. Y. Wang, J. Z. Guo, S. Y. Li, S. L. Mao, Y. Y. Lu, *Mater. Today Energy* **2022**, *26*, 100984; b) S. F. Song, W. L. Gao, G. M. Yang, Y. F. Zhai, J. Y. Yao, L. Y. Lin, W. P. Tang, N. Hu, L. Lu, *Mater. Today Energy* **2022**, *23*, 100893.

[44] Z. C. Li, W. H. Tang, Y. R. Deng, M. M. Zhou, X. D. Wang, R. P. Liu, C. A. Wang, *J. Mater. Chem. A* **2022**, *10*, 23047.

[45] J. Q. Wei, H. Y. Yue, Z. P. Shi, Z. Y. Li, X. N. Li, Y. H. Yin, S. T. Yang, *ACS Appl. Mater. Interfaces* **2021**, *13*, 32486–32494.

[46] a) Q. Liu, J. Tan, Z. F. Liu, X. Hu, J. H. Yu, X. S. Wang, J. R. Wu, B. Y. Cai, Q. Wang, Y. Z. Fu, H. B. Liu, B. H. Li, *ACS Appl. Mater. Interfaces* **2022**, *14*, 26612–26621; b) Y. J. Yang, R. Wang, J. X. Xue, F. Q. Liu, J. Yan, S. X. Jia, T. Q. Xiang, H. Huo, J. J. Zhou, L. Li, *J. Mater. Chem. A* **2021**, *9*, 27390–27397; c) D. L. Chen, M. Zhu, P. B. Kang, T. Zhu, H. C. Yuan, J. L. Lan, X. P. Yang, G. Sui, *Adv. Sci.* **2022**, *9*, 2103663.

[47] a) F. L. Zhou, H. Y. Liao, Z. Z. Zhang, *Ionics* **2020**, *26*, 3893–3900; b) T. W. Zhang, J. Zhang, S. Yang, Y. Li, R. Dong, J. L. Yuan, Y. X. Liu, Z. G. Wu, Y. Song, Y. J. Zhong, W. Xiang, Y. X. Chen, B. H. Zhong, X. D. Guo, *ACS Appl. Mater. Interfaces* **2021**, *13*, 44497–44508; c) W. Zhang, T. Ryu, S. Yoon, L. Jin, G. Jang, W. Bae, W. Kim, F. Ahmed, H. Jang, *Membranes* **2022**, *12*, 439.

[48] J. Yu, X. D. Lin, J. P. Liu, J. T. T. Yu, M. J. Robson, G. D. Zhou, H. M. Law, H. R. Wang, B. Z. Tang, F. Ciucci, *Adv. Energy Mater.* **2022**, *12*, 2102932.

[49] S. S. Wang, L. Zhou, M. K. Tufail, L. Yang, P. F. Zhai, R. J. Chen, W. Yang, *Chem. Eng. J.* **2021**, *415*, 128846.

[50] a) Y. S. Lee, D. W. Kim, *Electrochim. Acta* **2013**, *106*, 460–464; b) Y. C. Tseng, S. H. Hsiang, C. H. Tsao, H. S. Teng, S. S. Hou, J. S. Jan, *J. Mater. Chem. A* **2021**, *9*, 5796–5806; c) J. Y. Ma, X. Y. Ma, H. P. Zhang, F. Chen, X. H. Guan, J. P. Niu, X. P. Hu, *J. Membr. Sci.* **2022**, *659*, 120811; d) D. Zhou, R. L. Liu, J. Zhang, X. G. Qi, Y. B. He, B. H. Li, Q. H. Yang, Y. S. Hu, F. Y. Kang, *Nano Energy* **2017**, *33*, 45–54.

[51] a) M. E. Taylor, D. Clarkson, S. G. Greenbaum, M. J. Panzer, *ACS Appl. Polym. Mater.* **2021**, *3*, 2635–2645; b) Y. C. Tseng, S. H. Hsiang, T. Y. Lee, H. S. Teng, J. S. Jan, T. Kyu, *ACS Appl. Energ. Mater.* **2021**, *4*, 14309–14322; c) W. Choi, G. H. Sung, W. R. Yu, D. W. Kim, *ACS Appl. Energ. Mater.* **2022**, *5*, 8381–8390.

[52] X. T. Li, X. Q. Han, H. R. Zhang, R. X. Hu, X. F. Du, P. Wang, B. T. Zhang, G. L. Cui, *ACS Appl. Mater. Interfaces* **2020**, *12*, 51374–51386.

[53] T. Huang, M. C. Long, G. Wu, Y. Z. Wang, X. L. Wang, *ChemElectroChem* **2019**, *6*, 3674–3683.

[54] a) Y. S. Kim, Y. G. Cho, D. Odkhuu, N. Park, H. K. Song, *Sci. Rep.* **2013**, *3*, 1917; b) D. Zhou, Y. B. He, Q. Cai, X. Y. Qin, B. H. Li, H. D. Du, Q. H. Yang, F. Y. Kang, *J. Mater. Chem. A* **2014**, *2*, 20059–20066; c) D. Zhou, Y. B. He, R. L. Liu, M. Liu, H. D. Du, B. H. Li, Q. Cai, Q. H. Yang, F. Y. Kang, *Adv. Energy Mater.* **2015**, *5*, 1500353; d) E. Y. Zhao, S. Q. Luo, Z. X. Zhang, N. Saito, L. Yang, S. l. Hirano, *Electrochim. Acta* **2022**, *434*, 141299.

[55] H. Y. Guan, F. Lian, K. Xi, Y. Ren, J. L. Sun, R. V. Kumar, *J. Power Sources* **2014**, *245*, 95–100.

[56] K. W. Liu, S. Jiang, T. L. Dzwiniel, H. K. Kim, Z. Yu, N. L. D. Rago, J. J. Kim, T. T. Fister, J. Z. Yang, Q. Liu, J. Gilbert, L. Cheng, V. Srinivasan, Z. C. Zhang, C. Liao, *ACS Appl. Mater. Interfaces* **2020**, *12*, 29162–29172.

[57] H. L. Chen, P. He, M. Li, Y. H. Wen, Y. Wang, J. Y. Qiu, G. P. Cao, P. C. Zhao, S. T. Zhang, H. Ming, *ACS Appl. Energ. Mater.* **2022**, *5*, 5170–5181.

[58] Z. Y. Wen, Z. K. Zhao, L. Li, Z. Y. Sun, N. Chen, Y. J. Li, F. Wu, R. J. Chen, *Adv. Funct. Mater.* **2022**, *32*, 2109184.

[59] X. X. Jiao, J. Wang, G. X. Gao, X. Z. Zhang, C. M. Fu, L. N. Wang, Y. G. Wang, T. X. Liu, *ACS Appl. Mater. Interfaces* **2021**, *13*, 60054–60062.

[60] T. Y. Wang, Y. B. Li, J. Q. Zhang, K. Yan, P. Jaumaux, J. Yang, C. Y. Wang, D. Shanmukaraj, B. Sun, M. Armand, Y. Cui, G. X. Wang, *Nat. Commun.* **2020**, *11*, 5429.

[61] W. Fan, N. W. Li, X. L. Zhang, S. Y. Zhao, R. Cao, Y. Y. Yin, Y. Xing, J. N. Wang, Y. G. Guo, C. J. Li, *Adv. Sci.* **2018**, *5*, 1800559.

[62] Q. Liu, J. Tan, Z. F. Liu, X. Hu, J. H. Yu, X. S. Wang, J. R. Wu, B. Y. Cai, Q. Wang, Y. Z. Fu, H. B. Liu, B. H. Li, *ACS Appl. Mater. Interfaces* **2022**, *14*, 26612–26621.

[63] Y. He, H. J. Li, S. K. Huo, Y. Z. Chen, Y. F. Zhang, Y. Y. Wang, W. W. Cai, D. L. Zeng, C. Li, H. S. Cheng, *J. Power Sources* **2021**, *490*, 229545.

[64] Q. F. Sun, S. Wang, Y. Ma, Y. Zhou, D. W. Song, H. Z. Zhang, X. X. Shi, C. L. Li, L. Q. Zhang, *Energy Storage Mater.* **2022**, *44*, 537–546.

[65] T. Zhu, G. Q. Liu, D. L. Chen, J. X. Chen, P. Qi, J. Sun, S. Zhang, *Energy Storage Mater.* **2022**, *50*, 495–504.

[66] T. Huang, M. C. Long, X. L. Wang, G. Wu, Y. Z. Wang, *Chem. Eng. J.* **2019**, *375*.

[67] C. Ma, X. Y. Ni, Y. Q. Zhang, Q. B. Xia, L. J. Zhou, L. B. Chen, Y. G. Lai, X. B. Ji, C. L. Yan, W. F. Wei, *Matter* **2022**, *5*, 2225–2237.

[68] M. Liu, H. R. Jiang, Y. X. Ren, D. Zhou, F. Y. Kang, T. S. Zhao, *Electrochim. Acta* **2016**, *213*, 871–878.

[69] Z. N. Man, H. Tian, X. B. Zhu, Y. Wang, Y. G. Wu, X. Y. Wen, Z. Lu, *J. Electrochem. Soc.* **2022**, *169*, 060507.

[70] J. Pan, H. P. Li, H. Sun, Y. Zhang, L. Wang, M. Liao, X. M. Sun, H. S. Peng, *Small* **2018**, *14*, 1703454.

[71] J. J. Li, Z. C. Wang, L. Yang, Y. H. Liu, Y. L. Xing, S. C. Zhang, H. Z. Xu, *ACS Appl. Mater. Interfaces* **2021**, *13*, 18627–18637.